CellPress
Partner Journal

Molecular Plant
Research article

A decoy receptor derived from alternative splicing fine-tunes cytokinin signaling in *Arabidopsis*

Michaela Králová[1,6], Ivona Kubalová[2,6], Jakub Hajný[1], Karolina Kubiasová[3], Karolína Vagaská[1], Zengxiang Ge[3], Michelle Gallei[3], Hana Semerádová[3], Anna Kuchařová[1], Martin Hönig[4], Aline Monzer[3], Martin Kovačik[5], Jiří Friml[3], Ondřej Novák[1], Eva Benková[3], Yoshihisa Ikeda[2] and David Zalabák[1,*]

[1]Laboratory of Growth Regulators, Faculty of Science of Palacký University and Institute of Experimental Botany AS CR, Šlechtitelů 27, 783 71 Olomouc, Czech Republic

[2]Department of Molecular Biology, Centre of the Region Haná for Biotechnological and Agricultural Research, Faculty of Science, Palacký University, Šlechtitelů 27, 783 71 Olomouc, Czech Republic

[3]Institute of Science and Technology Austria (ISTA), 3400 Klosterneuburg, Austria

[4]Department of Chemical Biology, Faculty of Science, Palacký University, Šlechtitelů 27, 783 71 Olomouc, Czech Republic

[5]Institute of Experimental Botany of the Czech Academy of Sciences, Centre of Plant Structural and Functional Genomics, Šlechtitelů 31, 779 00 Olomouc, Czech Republic

[6]These authors contributed equally to this article.

***Correspondence: David Zalabák (david.zalabak@upol.cz)**

https://doi.org/10.1016/j.molp.2024.11.001

ABSTRACT

Hormone perception and signaling pathways have a fundamental regulatory function in the physiological processes of plants. Cytokinins, a class of plant hormones, regulate cell division and meristem maintenance. The cytokinin signaling pathway is well established in the model plant *Arabidopsis thaliana*. Several negative feedback mechanisms, tightly controlling cytokinin signaling output, have been described previously. In this study, we identified a new feedback mechanism executed through alternative splicing of the cytokinin receptor AHK4/CRE1. A novel splicing variant named *CRE1^{int7}* results from seventh intron retention, introducing a premature termination codon in the transcript. We showed that *CRE1^{int7}* is translated *in planta* into a truncated receptor lacking the C-terminal receiver domain essential for signal transduction. CRE1^{int7} can bind cytokinin but cannot activate the downstream cascade. We present a novel negative feedback mechanism of the cytokinin signaling pathway, facilitated by a decoy receptor that can inactivate canonical cytokinin receptors via dimerization and compete with them for ligand binding. Ensuring proper plant growth and development requires precise control of the cytokinin signaling pathway at several levels. CRE1^{int7} represents a so-far unknown mechanism for fine-tuning the cytokinin signaling pathway in *Arabidopsis*.

Králová M., Kubalová I., Hajný J., Kubiasová K., Vagaská K., Ge Z., Gallei M., Semerádová H., Kuchařová A., Hönig M., Monzer A., Kovačik M., Friml J., Novák O., Benková E., Ikeda Y., and Zalabák D. (2024). A decoy receptor derived from alternative splicing fine-tunes cytokinin signaling in *Arabidopsis*. Mol. Plant. **17**, 1850–1865.

INTRODUCTION

Cell signaling is a fundamental feature of all living organisms, allowing them to respond promptly to extracellular or intracellular signals. The signal inputs can be of a chemical nature (ligands, hormones, or other small molecules) or physical (e.g., temperature, light, pressure, or wounding). The signal is perceived by receptors and transduced via the activated signaling cascade to trigger cellular responses (Takeuchi et al., 2021).

The signaling pathways are stringently controlled at multiple levels via negative feedback loops as part of the primary responses. Negative feedback loops maintain homeostasis by resetting the signaling and thus allow for prompt, strong, and transient responses. A typical component of negative feedback regulation is the expression of a repressor attenuating the signaling pathway. At the receptor level, ligand access to the receptor is controlled by its biosynthesis, degradation (reversible or irreversible deactivation), and transport or distribution, allowing turning the signaling on and off (Gordon et al., 2009; Ferrell, 2013; Lemmon et al., 2016).

Published by the Molecular Plant Shanghai Editorial Office in association with Cell Press, an imprint of Elsevier Inc., on behalf of CSPB and CEMPS, CAS.

Decoy receptors represent a unique fine-tuning mechanism that evolved in mammalian systems (Mantovani et al., 2001). A decoy receptor is capable of ligand binding but structurally unable to activate the signaling cascade, thus competing with canonical receptors for ligand binding and attenuating the signaling cascade. A typical representative of the decoy receptor is the interleukin 1 receptor type II (IL-1R2), counteracting the canonical IL-1R1 to attenuate the inflammatory reaction by competing for IL binding (Re et al., 1994). Decoy receptor 3 titrates the tumor necrosis factor (TNF) ligand and thus prevents its binding to the canonical TNF receptors to modulate apoptosis (Ashkenazi, 2002). The activity of vascular endothelial growth factor receptor 1, another decoy receptor, is essential for angiogenesis and vascular growth (Meyer et al., 2006). Reports proposing regulatory mechanisms involving decoy receptors acting *in planta* are rather scarce (Bar et al., 2010). So far, no decoy receptors have been identified as an alternative mechanism to control the activity of plant hormonal signaling pathways.

Cytokinins are essential plant hormones and regulators of cell proliferation, meristem activity, shoot and root branching, root vascular development, chloroplast maturation, and response to biotic and abiotic stresses (Werner and Schmülling, 2009).

The *Arabidopsis thaliana* genome encodes three cytokinin receptors: *ARABIDOPSIS HISTIDINE KINASE 2* (*AHK2*), *AHK3*, and *AHK4/CYTOKININ RESPONSE 1 (CRE1)/WOODEN LEG (WOL)* (Inoue et al., 2001). All three cytokinin receptors play an important role in plant development with partially redundant functions; e.g., root apical maintenance, root vasculature development, *de novo* organ formation, and shoot growth regulation (Mähönen et al., 2000, 2006b; Higuchi et al., 2004; Riefler et al., 2006). The cytokinin receptors are localized at the plasma membrane (PM) and endoplasmic reticulum (ER) (Caesar et al., 2011; Wulfetange et al., 2011; Kubiasová et al., 2020), with a ligand-binding domain facing the apoplast or ER lumen and a histidine kinase domain and a receiver domain exposed to the cytosol (Lomin et al., 2018).

The cytokinin signaling cascade is initiated upon ligand binding to the receptor's N-terminal cyclase/histidine kinase-associated sensor extracellular–CHASE domain, leading to a conformational change, allowing for ATP binding in the histidine kinase domain. The activated histidine kinase domain transfers a phosphate to the conserved aspartate residue within the C-terminal receiver domain. Five AHP (ARABIDOPSIS PHOSPHOTRANSMITTER1–5) proteins then transmit the phosphate from the receiver domain of the receptor to 1 of 11 type B RESPONSE REGULATORS (B-ARRs) (Sakai et al., 1998; Lohrman, 2001; Hosoda et al., 2002) members of the myeloblastosis (MYB) transcription factor family. Phosphorylated B-ARRs trigger the expression of primary response genes.

The cytokinin signaling pathway is tightly controlled through several negative feedback loops. Type A ARRs (A-ARRs) are induced by cytokinin (Brandstatter and Kieber, 1998; Sakakibara et al., 1998) and interfere with B-ARR activity. The exact molecular mechanism of A-ARR activity is unknown. There are two proposed hypothetical modes of action. The first scenario presumes that, although A-ARRs can receive a phosphate from activated AHPs, they lack a DNA-binding domain and cannot trigger gene expression, thus probably providing competitive inhibition of B-ARRs. The second scenario proposes that A-ARRs heterodimerize with B-ARRs and inactivate them (To et al., 2004). Other negative feedback mechanisms involve protein stabilization of A-ARRs upon cytokinin treatment (To et al., 2008); S-nitrosylation of AHP1, blocking its activation (Feng et al., 2013); proteasome-dependent degradation of B-ARRs (ARR2) by the KISS ME DEADLY ubiquitin E3 ligase complex (Kim et al., 2013); and induction of the cytokinin-degrading enzyme CYTOKININ OXIDASE (Werner et al., 2006). AHP6 uses its pseudo-phosphotransfer domain to stop the phosphorelay (Mähönen et al., 2006a). All of these mechanisms provide several layers of regulation to tightly control the cytokinin signaling essential for normal plant organ growth and development.

Here we identified an unknown mechanism of cytokinin signaling control mediated by a decoy receptor lacking the receiver domain essential for signal transduction. A decoy receptor is encoded by a transcript variant, called *CRE1^{int7}* hereafter, resulting from alternative splicing. Though CRE1^{int7} ligand binding is unaffected, it cannot activate the signaling cascade, thus providing competitive inhibition. We show that CRE1^{int7} localizes to the same subcellular compartments as the canonical CRE1 receptor and attenuates the signaling by interfering with cytokinin signal transduction *in planta*. Given that cytokinin enhances the accumulation of the *CRE1^{int7}* splicing variant, we propose that this mechanism facilitates resetting of the signaling cascade in plants when the level of active cytokinin increases; for example, in response to fluctuating nutrient availability (Takei et al., 2001; Sakakibara et al., 2006; Wendrich et al., 2020). This unknown mechanism represents another layer of cytokinin signaling control modulating plant developmental plasticity.

RESULTS

Cytokinin interferes with the splicing of the seventh intron of *CRE1*

The *CRE1* gene consists of 10 exons interrupted by 9 intron sequences (Figure 1A). The first intron of *CRE1* undergoes complex alternative splicing, generating six splice variants annotated in The Arabidopsis Information Resource database (www.arabidopsis.org). However, their role has yet to be elucidated. The first intron splicing presumably controls the CRE1 protein N terminus to modulate the receptor function.

When cloning a *CRE1* open reading frame (ORF), we isolated a previously undescribed transcript variant, *CRE1^{int7}*, produced via alternative splicing of the seventh *CRE1* intron. The *CRE1^{int7}* transcript was identified using the primers (F1+R1) for amplification of the region from initiation to the termination codon (Figure 1A; Supplemental Table 1). The template cDNA was prepared from Col-0 root explants cultured on a shoot-inducing medium. Sequencing of two independent clones revealed that the *CRE1* region contains a 78-bp-long retained seventh intron (Supplemental Figure 1B), while other introns were spliced out. Retention of the seventh intron introduces a premature termination codon (PTC), potentially resulting in a truncated protein lacking the receiver domain and affecting the

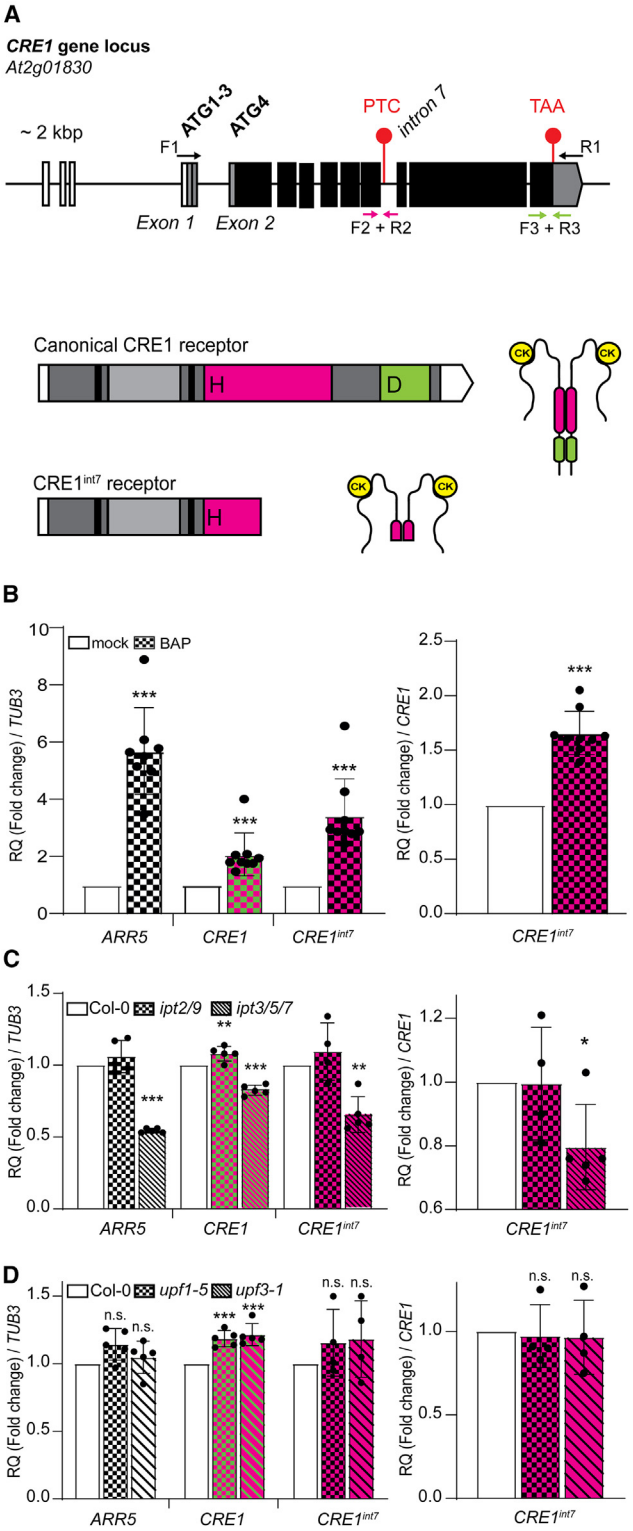

Figure 1. Alternative splicing of the *CRE1* gene produces the CRE1^{int7} receptor variant lacking the receiver domain.

(A) Structure of the *CRE1* gene. *CRE1* consists of 10 exons (rectangles) and 9 introns (lines). The transcript encoding the canonical *CRE1* receptor produced through constitutive splicing encodes the ligand-binding cyclase/histidine-kinase-associated sensor extracellular–CHASE domain (light gray) flanked by two transmembrane domains (black bars), followed by a histidine kinase domain (magenta) with a conserved histidine motif (H) and receiver domain (green) with conserved aspartic acid. The *CRE1*^{int7} variant resulting from alternative splicing retains intron 7, introducing a premature termination codon (PTC; red dot) into the *CRE1* transcript. *CRE1*^{int7} encodes the truncated receptor, which lacks a C-terminal part, including the conserved receiver domain. The 5′ and 3′ UTRs (white) and the canonical termination codon (TAA, red dot) are shown. Conformations of CRE1 and CRE1^{int7} receptors are shown (right). Primer pair F1+R1 was used for cloning the *CRE1* transcript from root explants and resulted in isolation of the *CRE1*^{int7} variant. The primer pair positions to detect *CRE1*^{int7} (F2 and R2) and overall *CRE1* transcripts (F3 and R3) used in RT-qPCR experiments are shown **(B)**.

(B–D) Expression analyses of *CRE1* and *CRE1*^{int7} in mock- and cytokinin-treated roots of Col-0 WT **(B)**, cytokinin biosynthesis mutants *ipt2/9* and *ipt3/5/7* **(C)**, and *upf1-5* and *upf3-1* mutants in the nonsense-mediated mRNA decay (NMD) pathway **(D)**. mRNA was isolated from roots of 4-day-old seedlings treated with cytokinin (1 μM BAP, 1 h) or DMSO (mock). RT-qPCR was performed using primer combinations F2-R2 and F3-R3 to monitor *CRE1*^{int7} and overall *CRE1* transcripts, respectively. The relative gene expression (RQ/*TUB3*) was normalized to *TUB3* (left). To figure out the effect of treatment or mutation on seventh intron splicing, the relative gene expression of *CRE1*^{int7} was also normalized to overall *CRE1* transcripts (RQ/*CRE1*) (right). Values are the mean from nine **(B)** and five **(C and D)** independent experiments. The *p* value shows the Student's *t*-test data comparing differences between mock and BAP **(B)** or mutants and Col-0 WT **(C and D)**. $^{*}p < 0.05$, $^{**}p < 0.01$, $^{***}p < 0.001$; n.s., non-significant. Results represent the mean value ± standard error.

receptor function (Figure 1A and Supplemental Figure 1B). We searched public databases and analyzed some available RNA sequencing datasets. In *Arabidopsis* root samples, we identified 2 sequencing reads (of 38 reads spanning the seventh *CRE1* intron) that mapped on the seventh intron, likely belonging to *CRE1*^{int7} transcripts (Supplemental Figure 1A). This bioinformatics analysis suggests that the abundance of *CRE1*^{int7} is rather low, up to 5% of all *CRE1* transcripts. We employed quantitative reverse transcription PCR (RT-qPCR) followed by absolute quantification to empirically verify these results.

RT-qPCR using the primer pair F3+R3 annealing within the last exon was employed to detect all *CRE1* transcript variants, while pair F2+R2 annealing to the seventh exon and intron specifically recognizes the *CRE1*^{int7} variant (Figure 1A and Supplemental Figure 1B; Supplemental Table 1). The specificity of RT-qPCR amplicons was verified by sequencing (Supplemental Figure 1C). To exclude the possibility of contamination with genomic DNA, the isolated RNA was tested using primers binding to the non-transcribed promoter region of *Ethylene Response Factor 8* (*ERF8*), a gene unrelated to *CRE1* (Supplemental Table 1). PCR amplification of the *ERF8* promoter region confirmed that there was no genomic DNA contamination, while diluted genomic DNA served as a positive control (Supplemental Figure 1D). The analysis confirmed that *Arabidopsis* roots contain 930 ± 187 *CRE1*^{int7} of 41 140 ± 3440 total *CRE1* transcripts (per 100 ng of total RNA), representing 2.3% of the *CRE1* transcript pool (Supplemental Figure 1E).

Since the shoot-inducing medium is enriched for cytokinins, we hypothesized that the retention of the seventh intron within the *CRE1* transcript might be cytokinin regulated. To address this question, we examined the levels of *CRE1* and *CRE1*^{int7} transcripts in response to cytokinin (1 μM 6-benzylaminopurine [BAP], 1 h) in

Arabidopsis roots. To assess the cytokinin effect on *CRE1* expression, we performed a relative quantification (RQ) by normalizing the target gene expression to the housekeeping gene *TUBULIN 3* (RQ/*TUB3).*

The expression of both *CRE1* as well as *CRE1^{int7}* transcripts increased with cytokinin treatment (1 μM BAP, 1 h) when compared to mock-treated roots; the cytokinin treatment promoted *CRE1^{int7}* transcripts more strongly than those of *CRE1* (Figure 1B). To distinguish whether *CRE1^{int7}* increased due to cytokinin-induced transcription or via cytokinin-regulated intron retention, we normalized the *CRE1^{int7}* expression (F2+R2) to total *CRE1* transcripts (F3+R3) presented as fold change RQ/*CRE1*. The RQ/*CRE1* fold change of *CRE1^{int7}* increased when compared to mock-treated roots (Figure 1B). These results suggest that cytokinin likely affects the splicing of the seventh *CRE1* intron, which leads to the accumulation of *CRE1^{int7}* transcripts.

To assess the effect of endogenous cytokinins on *CRE1^{int7}* splicing, we employed *ipt3/5/7* and *ipt2/9*, mutants of the cytokinin biosynthesis gene *ISOPENTENYL TRANSFERASE*. The levels of isopentenyl adenine (iP) and *trans*-zeatin (*t*Z), the most bioactive cytokinin forms, and their corresponding metabolites are decreased in *ipt3/5/7* (Miyawaki et al., 2006), as manifested by reduced transcription of *ARR5*, the cytokinin primary response gene, when compared to Col-0 wild-type (WT) roots (Figure 1C). On the other hand, the mutant *ipt2/9* lacks tRNA-derived cytokinins, which are biologically less active *cis*-zeatin *c*Z types (Miyawaki et al., 2006); thus, no dramatic alteration in *ARR5* expression is observed in this mutant background (Figure 1C). Analyses of *CRE1* transcript variants revealed a stronger reduction of *CRE1^{int7}* when compared to *CRE1* transcripts in the *ipt3/5/7* mutant, which resulted in a significantly lower RQ/*CRE1* fold change of *CRE1^{int7}* (Figure 1C). Unlike in *ipt3/5/7*, expression of the *CRE1* transcript variants and RQ/*CRE1* fold change of *CRE1^{int7}* did not change in the *ipt2/9* double mutant (Figure 1C). These results suggest that *CRE1^{int7}* splicing is controlled by the level of active cytokinins, which are preferentially perceived by CRE1 with high specificity (Yamada et al., 2001).

Aberrant mRNA transcripts are recognized by the nonsense-mediated mRNA decay pathway (NMD pathway) and targeted for degradation, since their detrimental function represents a potential risk for the organism (Arciga-Reyes et al., 2006). To examine the biological relevance of *CRE1^{int7}* transcript formation, we analyzed the expression level as well as the splicing index of *CRE1^{int7}* in *upf1-5* and *upf3-1* loss-of-function mutants deficient in critical components of the NMD machinery in *Arabidopsis* (Arciga-Reyes et al., 2006). Although *CRE1* expression is slightly increased in *upf1-5* and *upf3-1* mutants, the RQ/*CRE1* fold change of *CRE1^{int7}* is unchanged (Figure 1D), suggesting that *CRE1^{int7}* is not a substrate of the NMD pathway and is expected to have a biological function.

CRE1^{int7} can bind cytokinin but cannot activate the signaling cascade

To explore the impact of the seventh intron retention on CRE1 receptor function, we analyzed the ligand-binding capacity of both CRE1 variants in an *E. coli* expression system (Romanov et al., 2005). This assay is based on the competition of the tritiated ligand [^{3}H]*t*Z bound to the receptor protein with unlabeled cytokinins (iP, *t*Z). If the protein can bind the ligand, then the [^{3}H]*t*Z is displaced by unlabeled iP and *t*Z, decreasing the counts per unit signal. Unlabeled 10 μM *t*Z and iP comparably displaced the 3 nM [^{3}H]*t*Z from both receptor proteins in 30 min, accompanied by decreased counts per unit levels, suggesting that both receptor variants display similar affinity to cytokinins (Figure 2A). The control culture, carrying an empty expression plasmid, showed only a weak background signal, corroborating the specificity of CRE1 ligand binding (Figure 2A).

Next, we evaluated the ability of both receptor variants to initiate the transduction cascade following cytokinin binding. To achieve this, we used an established *E. coli* YojN→RcsB→cps::*lacZ* expression system, which allows the functional activity of receptors to be measured using β-galactosidase (*lacZ*) activity as a readout (Suzuki et al., 2001). *E. coli* expressing canonical *CRE1* (Supplemental Figure 2A) displayed a significant increase in β-galactosidase reporter activity when compared to bacteria transformed with an empty vector after cytokinin treatment (1 μM iP, 6 h) (Figure 2B). Notably, application of cytokinin to *E. coli* expressing the *CRE1^{int7}* variant (Supplemental Figure 2A) did not enhance reporter activity above the background level (Figure 2B). These experiments showed that the CRE1^{int7} variant retains the ligand-binding capacity but cannot transmit the signal downstream of the signaling cascade.

CRE1^{int7} attenuates cytokinin signaling

To test the function of CRE1^{int7} *in planta*, we used a *TCS::LUC* (*TWO-COMPONENT SYSTEM::LUCIFERASE*) assay in *Arabidopsis* protoplasts (Müller and Sheen, 2008), an established transient reporter system to monitor cytokinin output. The *CRE1* variants were C-terminally fused with *GFP* (*GREEN FLUORESCENT PROTEIN*) driven by the constitutive *CaMV35S* (*Cauliflower Mosaic Virus 35S*) promoter and co-expressed with the *TCS::LUC* cytokinin-sensitive reporter in protoplasts isolated from Col-0 root suspension culture. In control Col-0 protoplasts expressing only free GFP from the *CaMV35S* promoter, the relative luciferase activity increased 17.8 ± 2.13 times upon cytokinin treatment (500 nM BAP, 12 h) when compared to mock treatment (Figure 2C). This background activity is attributed to the native cytokinin signaling machinery present in Col-0 WT protoplasts. The cytokinin response was significantly increased in protoplasts expressing the canonical CRE1-GFP. In protoplasts co-transfected with *CRE1-GFP* and the *TCS::LUC* reporter, cytokinin enhanced luciferase activity 27.8 ± 0.82 times when compared to mock treatment. In contrast, after co-expression of *CRE1^{int7}-GFP* with the *TCS::LUC* reporter, cytokinin enhanced the luciferase activity 7.1 ± 1.40 times when compared to mock treatment (Figure 2C). Hence, protoplasts expressing CRE1^{int7}-GFP demonstrated a 60% reduction in relative luciferase activity in response to cytokinin compared to protoplasts expressing free GFP. This significantly weaker cytokinin signaling response in protoplasts expressing CRE1^{int7} when compared to those transformed with GFP control plasmid indicates that CRE1^{int7} interferes with and attenuates the activity of the native cytokinin signaling machinery present in cells.

Both variants of CRE1-GFP proteins co-localized with the ER marker AtWAK2-tdTomato-HDEL (Gomord et al., 1997;

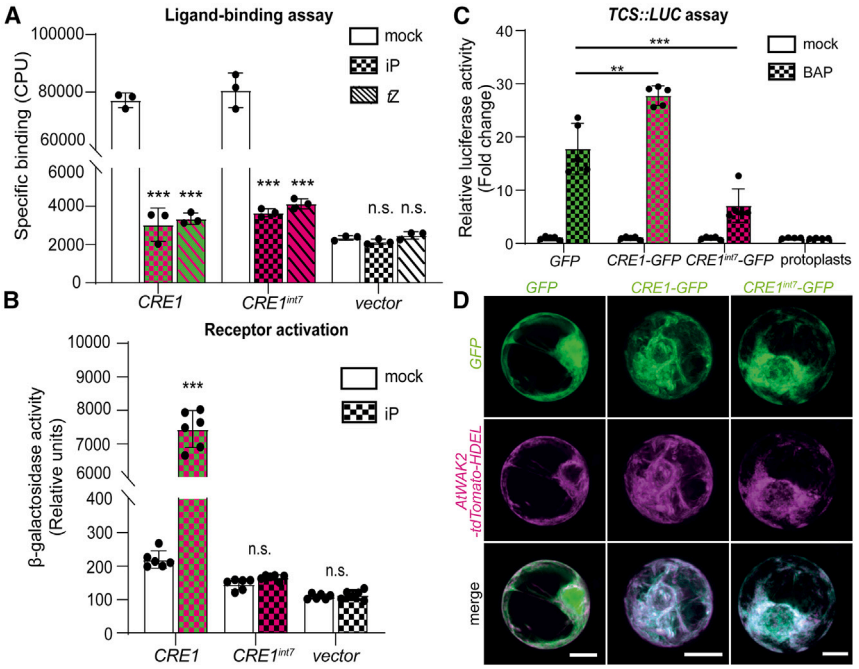

Figure 2. CRE1^{int7} binds cytokinin but does not activate the signaling pathway.

(A) Competitive ligand binding assay in *E. coli* expressing *CRE1*, *CRE1^{int7}*, and the *pIN-III_4xMyc_tNOS* vector (vector). The specific binding of 3 nM [2-^{3}H]*t*Z was examined in a competitive assay using unlabeled 10 μM iP and *t*Z. Values show the mean from three biological replicates ± standard deviation. The *p* value shows the Student's *t*-test differences between mock and iP or *t*Z, respectively; ***$p < 0.001$.

(B) Receptor activation assay in *E. coli* KMI001 expressing CRE1 and CRE1^{int7} receptors. ß-Galactosidase activity was measured in mock-treated (DMSO, 0.1%) and cytokinin-treated (1 μM iP, 6 h) treated. The values represent the mean from six biological replicates ± standard deviation. The *p* value shows the Student's *t*-test, with the differences between mock and iP compared. ***$p < 0.001$.

(C) *TCS::LUC* (*TWO-COMPONENT SYSTEM::LUCIFERASE*) assay in *Arabidopsis* protoplasts. *CRE1-GFP*, *CRE1^{int7}-GFP*, or free *GFP* was co-expressed with the *TCS::LUC* reporter in protoplasts isolated from Col-0 root suspension culture. Luciferase activity was measured after mock (DMSO) or cytokinin (500 nM BAP, 12 h) treatment. The values represent the mean from five biological replicates ± standard deviation. The *p* value shows the Student's *t*-test; *CRE1-GFP*, and *CRE1^{int7}-GFP* were compared to *GFP* control. **$p < 0.01$, ***$p < 0.001$.

(D) Expression of *CaMV35S::CRE1-GFP*, *CaMV35S::CRE1^{int7}-GFP*, and *CaMV35S::GFP* in *Arabidopsis* Col-0 protoplasts (green). Protoplasts were co-transformed with *AtWAK2-tdTomato-HDEL* (ER marker, magenta). Maximum-intensity projection of at least five Z sections of protoplasts is shown. Representative images are presented. Scale bars, 10 μm.

He et al., 1999) in Col-0 protoplasts (Figure 2D). The localization pattern, as well as the signal intensity, were comparable between CRE1-GFP and CRE1^{int7}-GFP, implying that both variants act in the same compartments. The expression of both CRE1 protein variants was verified using western blotting. Apart from bands of the expected sizes of 148 and 93 kDa, corresponding to CRE1-GFP and CRE1^{int7}-GFP monomers, respectively, we also detected 296 and 186 kDa bands corresponding to receptor dimers, confirming that GFP is not cleaved from CRE1 proteins and that both proteins dimerize (Supplemental Figure 2B). Altogether, the results support the CRE1^{int7} function as a decoy receptor attenuating the cytokinin signaling output.

CRE1^{int7} acts as a decoy receptor to quench cytokinin signal transduction *in planta*

To explore the functions of both CRE1 variants *in planta*, we generated transgenic *Arabidopsis* lines expressing *CRE1-GFP* and *CRE1^{int7}-GFP* under the control of the 2 kbp native *CRE1* promoter followed by the *TMVΩ* translational enhancer. These constructs allow for tissue-specific overexpression (Michniewicz et al., 2015). Both fusion proteins are predominantly expressed in tissues of the root stele, including phloem cells, xylem cells, and intervening cambial cells (Figures 3A and 3B). The strong expression was also detected during the early stages of lateral root (LR) formation, and it persisted during LR emergence (Figure 3C). The CRE1-GFP as well as CRE1^{int7}-GFP fusion proteins showed an ER localization pattern and accumulated at the PM in cells of the root stele (Figures 3A and 3B). This is in agreement with the previously reported CRE1 tissue-specific expression (Mähönen et al., 2000; Higuchi et al., 2004) and localization patterns (Antoniadi et al., 2020; Kubiasová et al., 2020).

To compare the role of receptor variants in plant development, we examined the root systems of transgenic lines expressing *pCRE1::CRE1-GFP* and *pCRE1::CRE1^{int7}-GFP* in *cre1-2* and Col-0, respectively. Lines with *pCRE1::GFP* transformed into *cre1-2* and Col-0 WT backgrounds were used as controls. Cytokinin is a well-established negative hormonal regulator of the root system (Auer, 1996). The exogenous application of cytokinin at nanomolar concentrations (50 nM BAP) suppressed the primary root growth and LR development in the Col-0 WT (Figure 4A and 4C). The *cre1-2* null mutant displayed substantially decreased cytokinin sensitivity (Inoue et al., 2001) when compared to the Col-0 WT (Figures 4A and 4B). While cytokinin (50 nM BAP) inhibited the primary root growth of 8-day-old seedlings in Col-0 by 22%, in *cre1-2,* it was only by 9%, proving that it is cytokinin hyposensitive (Figure 4B).

The roots of the *pCRE1::CRE1^{int7}-GFP,*Col-0 seedlings were significantly less sensitive to cytokinin when compared to Col-0 and *pCRE1::GFP*,Col-0 control seedlings. The cytokinin application inhibited primary root growth of three independent *pCRE1::CRE1^{int7}-GFP*,Col-0 lines only by 0%–11%, while in *pCRE1::GFP*,Col-0, it was by 19%–21% (Figure 4A and 4B). Furthermore, similar to the *cre1-2* mutant (20.3 LRs/root), roots of *pCRE1::CRE1^{int7}-GFP*,Col-0 formed 16.6–26 LRs in the presence of cytokinin (Figure 4C). Cytokinin application decreased the LR density in all tested lines, including the *cre1-2* mutant (Figure 4D). Only one independent line of *pCRE1::CRE1^{int7}-GFP*,Col-0 showed increased LR density upon cytokinin

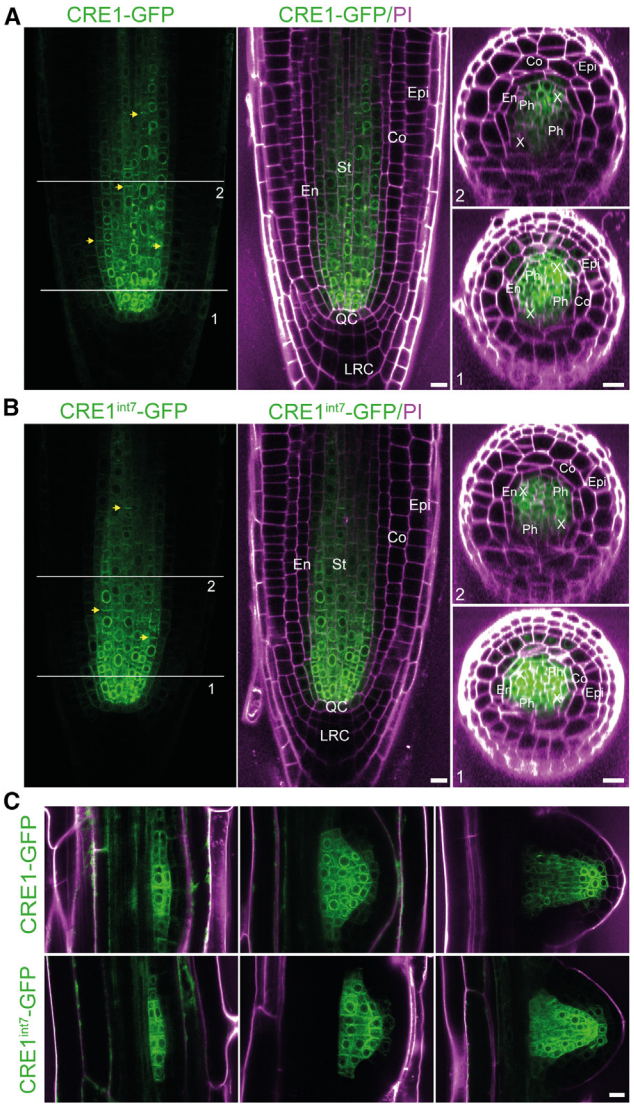

Figure 3. CRE1 and CRE1^{int7} are expressed in the root stele and LR primordia.

Shown is expression of *pCRE1::CRE1-GFP* **(A)** and *pCRE1::CRE1^{int7}-GFP* **(B)** in primary roots **(A and B)** and LRs **(C)** of 5- and 6-day-old seedlings, respectively. Shown are a longitudinal section through the primary root central zone (left, middle) and cross-sections through the root apical meristem in two positions. Horizontal lines 1 and 2 indicate the position of the focal plane of individual root cross-sections **(A and B)**. Shown are the CRE1-GFP (top) and CRE1^{int7}-GFP (bottom) signals in three developmental stages of LRs **(C)**. En, endodermis; St, stele; Co, cortex; Epi, epidermis; X, xylem; Ph, phloem; QC, quiescent center; LRC, lateral root cap. CRE1-GFP **(A)** and CRE1^{int7}-GFP **(B)** signal in the PM (yellow arrows) are shown. Magenta, propidium iodide; green, GFP. At least 15 individual roots were imaged. Scale bars, 10 μm.

application when compared to the Col-0 WT and *cre1-2* (Figure 4D). These observations demonstrate that CRE1^{int7}-GFP interferes with endogenous canonical receptors, ultimately decreasing the sensitivity of roots to cytokinin.

Furthermore, *pCRE1::CRE1^{int7}-GFP*,Col-0 seedlings grown on the mock medium showed longer primary roots during the first 7 days of growth when compared to the control lines and complementation lines (Supplemental Figure 3A and 3B). The seeds of *pCRE1::CRE1^{int7}-GFP*,Col-0 germinate about 4 h earlier when compared to the Col-0 WT and *cre1-2* mutant and 5 h earlier when compared to the *pCRE1::CRE1-GFP,cre1-2* line (Supplemental Figure 3C).

Next, the expression of three cytokinin primary response genes *ARR5, ARR7*, and *ARR16* was significantly lowered in the *pCRE1::CRE1^{int7}-GFP*,Col-0 line compared to the Col-0 WT and even to the *cre1-2* null allele mutant upon cytokinin application (Supplemental Figure 4A). These results further support the role of CRE1^{int7} in cytokinin signaling attenuation.

Transgenes often undergo epigenetic silencing through mechanisms of transcriptional gene silencing (TGS) or post-transcriptional gene silencing (PTGS). Both mechanisms can lead to *cis*-inactivation of transgenes or *trans*-inactivation of endogenous homologous genes (Rajeevkumar et al., 2015). To investigate whether the phenotype of *pCRE1::CRE1^{int7}-GFP*,Col-0 plants is caused by silencing of the endogenous *CRE1* gene, we monitored the expression of the native *CRE1* transcripts in this line and found it to be unchanged (Supplemental Figure 4B). This finding confirms that the observed phenotype of the CRE1^{int7}-expressing line is not affected by transgene silencing.

The construct *pCRE1::CRE1-GFP* was introduced into the *cre1-2* mutant background, and the rescue of phenotype was analyzed on a medium supplemented with cytokinin (50 nM BAP; Supplemental Figure 5A and 5B). The primary root growth inhibition of four independent *pCRE1::CRE1-GFP,cre1-2* lines ranged from 34% to 47% and, thus, was comparable to the 10-day-old seedlings of the Col-0 WT (35% inhibition). Notably, the number of LRs on 12-day-old *pCRE1::CRE1-GFP,cre1-2,* and Col-0 seedlings grown on a cytokinin-containing medium decreased to 3.1 and 6.5, unlike the *cre1-2* mutant, in which 16.8 LRs per root were observed (Supplemental Figure 5C). Similarly, the LR density was significantly decreased in all four independent *pCRE1::CRE1-GFP,cre1-2* lines upon cytokinin treatment and was comparable to Col-0 WT seedlings (Supplemental Figure 5D). These results show that the *pCRE1::CRE1-GFP* construct complements the *cre1-2* mutant root phenotype.

CRE1^{int7} dimerizes with canonical AHK receptors

To explore the function of the *CRE1^{int7}* transcript in better detail, we introduced *pCRE1::CRE1^{int7}-GFP* into the *cre1-2* mutant background by crossing. During the selection process, we easily obtained plants homozygous for CRE1^{int7}-GFP and heterozygous for *cre1-2* but repeatedly failed to isolate seedlings homozygous for both alleles. This led us to the assumption that the homozygous combination might be embryonic lethal. Therefore, we harvested the individual siliques of the heterozygote plant, plated the complete set of seeds on Murashige and Skoog (MS) medium, and analyzed the phenotype of the offspring (Supplemental Figure 6A). We observed dwarfed seedlings segregating at a 25% ratio. The genotyping of these individuals confirmed that they were homozygous for both alleles (Supplemental Figure 6B). The dwarfed homozygous seedlings did not survive transfer into the soil and could not be propagated. The microscopic analysis confirmed that the proliferation of root vascular cells is

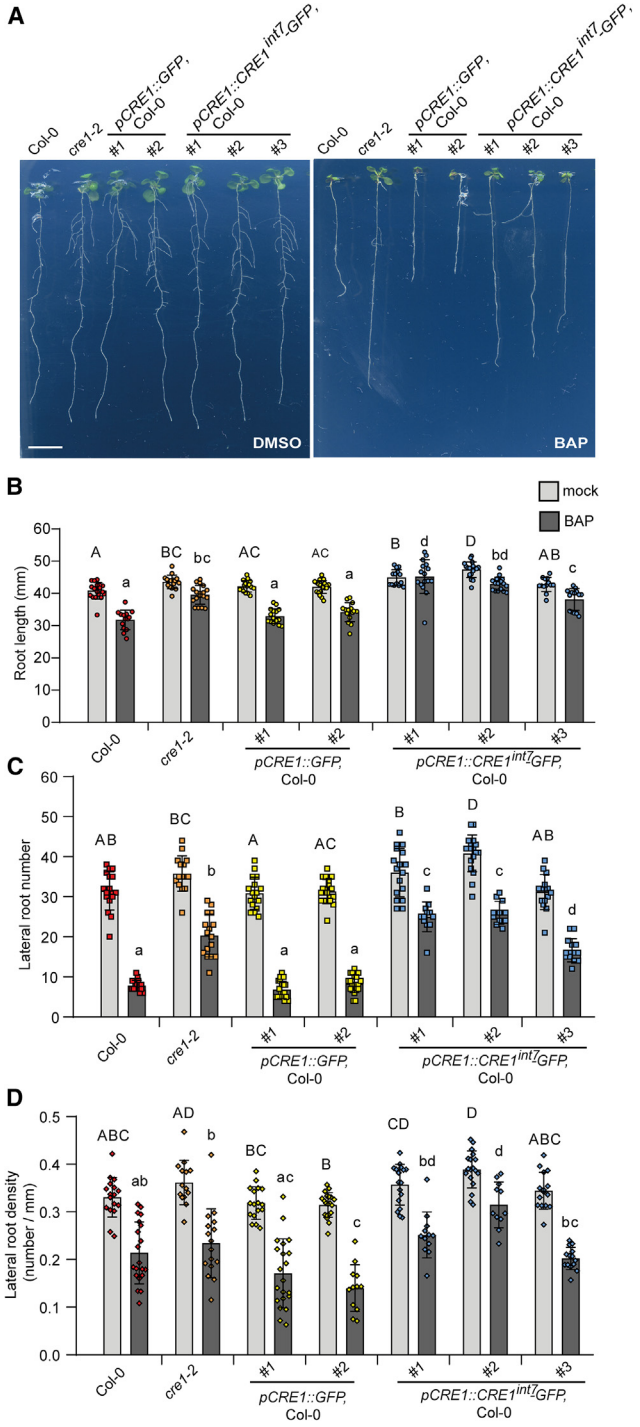

Figure 4. *Arabidopsis* seedlings expressing CRE1^{int7}-GFP are less sensitive to cytokinin.

Shown are seedlings of Col-0, *cre1-2*, *pCRE1::GFP*,Col-0 (controls, two independent lines) and *pCRE1::CRE1^{int7}-GFP*,Col-0 (three independent lines) on control (DMSO, left) and cytokinin-containing (BAP, right) medium **(A)**. Seedlings were grown for 5 days on MS medium, transferred to MS medium supplemented with cytokinin (50 nM BAP) or DMSO (mock control), and grown for an additional 7 days. Primary root length **(B)** was evaluated 8 days after germination, while the number of emerged lateral roots (LRs) per root **(C)** and LR density **(D)** were evaluated 12 days after germination. Results represent means ± standard deviation ($n \geq 12$). A parametric one-way ANOVA was used to compare the differences between groups, followed by Tukey's multiple-comparisons test for post hoc analysis ($p < 0.05$). Data comparing differences between Col-0 WT and respective transgenic lines are shown. Treatment results are differentiated typographically/ A, mock; a, 50 nM BAP. The experiment was repeated three times with similar results. The graph represents the results from one experiment. Scale bar, 1 cm.

strongly reduced in homozygotes when compared to the Col-0 WT (Supplemental Figure 6C). This phenotype resembled the *wooden leg* mutation (Mähönen et al., 2000) or phenotypes of the *ahk* triple receptor mutant (Riefler et al., 2006).

To figure out what causes such a pronounced phenotype, we explored the cytokinin primary response genes in this cross. Since the homozygotes were nonviable, we analyzed the expression in progenies of the heterozygous line *pCRE1::CRE1^{int7}-GFP*(+/+),*cre1-2*(+/−). The expression of *ARR5*, *ARR7*, and *ARR16* was unaffected in nontreated *pCRE1::CRE1^{int7}-GFP*(+/+),*cre1-2*(+/−) plants (Supplemental Figure 4A) but decreased upon cytokinin application when compared to Col-0 or the *cre1-2* null allele mutant (Supplemental Figure 4A). The expression of the endogenous *CRE1* gene was unaffected, similar to the CRE1^{int7}-GFP line (Supplemental Figure 4B), confirming that TGS and PTGS are not involved.

This result showed that CRE1^{int7} interferes with the cytokinin signaling machinery *in planta*. We decided to explore why the phenotype appears only in the *cre1-2* null mutant background. Since CRE1^{int7} can form homodimers *in planta* (Supplemental Figure 2B), we assumed that it might eventually dimerize with canonical CRE1 or AHK2 and AHK3 to inhibit their receptor activity. To test this hypothesis, we performed a bimolecular fluorescence complementation (BiFC) experiment. First, we prepared a new set of Gateway-compatible vectors with a split *mNeonGreen* reporter for expression in protoplasts (supplemental information). BiFC experiments confirmed that CRE1^{int7} can form homodimers and can also dimerize with all three canonical cytokinin receptors (Supplemental Figure 7A). Dimerization with canonical CRE1 was further validated by fluorescence resonance energy transfer/fluorescence lifetime imaging microscopy (FRET/FLIM) analysis (Supplemental Figure 7B).

The seventh intron negatively regulates CRE1 receptor function *in planta*

To dissect the effect of the seventh intron on CRE1 receptor function *in planta* in the context of cytokinin signaling, we prepared plants carrying the reporter construct *pCRE1::gCRE1$^{\Delta int7}$-GFP* lacking the seventh intron in the *CRE1* genomic sequence and analyzed their phenotype on a low concentration of BAP (20 and 50 nM). The corresponding control reporter, *pCRE1::gCRE1^{WT}-GFP*, containing the WT *CRE1* genomic sequence, was prepared for comparison. Both reporters express the same CRE1-GFP protein fusion. Lines with comparable CRE1-GFP expression were selected for these experiments (Supplemental Figure 8E). Two independent *pCRE1::gCRE1$^{\Delta int7}$-GFP* transgenic lines exhibited shorter primary roots on mock treatment when compared to *pCRE1::gCRE1^{WT}-GFP* controls. The sensitivity of both *pCRE1::gCRE1$^{\Delta int7}$-GFP* transgenic lines to BAP was higher, manifested by shorter primary roots compared to *pCRE1::gCRE1^{WT}-GFP.* The difference between

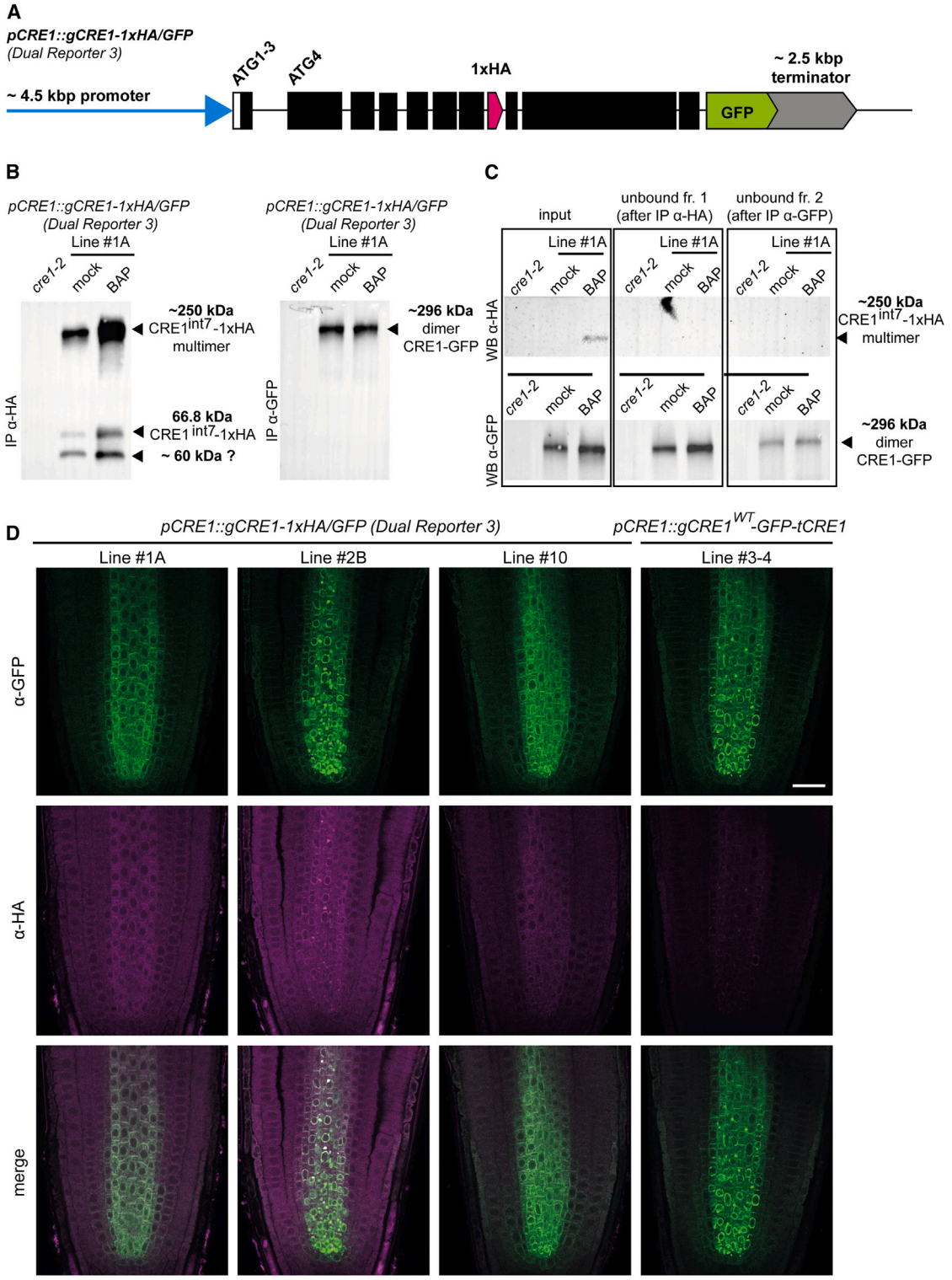

Figure 5. *CRE1^{int7}* transcripts are translated *in planta*.

(A) The genetic map of *pCRE1::gCRE1-1xHA/GFP* (DR 3). DR 3 was introduced into the *cre1-2* mutant background.

(B and C) Immunoprecipitation (IP) from *pCRE1::gCRE1-1xHA/GFP* (DR 3) line #1A. Five-day-old seedlings were grown vertically on MS medium and then transferred to liquid MS medium and treated with cytokinin (1 μM BAP) or DMSO solvent (mock) for 2 h. The CRE1^{int7}-1×HA protein was immunoprecipitated on anti-HA (α-HA) magnetic beads (left) from crude protein extract (input). The unbound proteins (unbound fraction 1) were consequently immunoprecipitated using anti-GFP (α-GFP). Here, CRE1-GFP proteins were pulled down (right).

(legend continued on next page)

pCRE1::gCRE1$^{\Delta int7}$-GFP and *pCRE1::gCRE1^{WT}-GFP* primary root lengths was modest but significant on both BAP concentrations (Supplemental Figure 8A and 8B). No phenotypic differences in LR number or LR density were observed between both reporters upon 20 nM or 50 nM BAP treatment (Supplemental Figure 8C and 8D).

CRE1^{int7} transcripts are translated *in planta*

To test whether CRE1^{int7} is translated *in planta*, we prepared a set of splicing reporters named dual reporters (DRs 1–3). The splicing reporters are commonly used in mammalian models but have only recently been used successfully *in planta* (Kashkan et al., 2022). In principle, the first reporter gene (e.g., *GFP*) is introduced in the region of the splicing event (before PTC in the intron), and the second reporter gene (e.g., *mCherry*) is inserted before the canonical termination codon (TAA). When intron retention occurs, *GFP* is in frame, and, thus, a green fluorescent signal can be detected *in planta*. When constitutive splicing occurs, the intron is spliced out (including *GFP*), and, as a consequence, *mCherry* is in frame with the canonical transcripts. Therefore, a red fluorescent signal can be observed *in planta*.

The main limitation is the short length of the plant introns. For instance, the seventh *CRE1* intron has only 78 bp. Insertion of the *GFP* reporter sequence, therefore, dramatically expands the intron size and changes the exon/intron proportion, possibly leading to intron missplicing (e.g., constitutive intron retention). This was also our case. Our first two attempts to prepare a functional *CRE1* splicing reporter failed (Supplemental Figure 9).

In the case of *pCRE1::gCRE1-GFP/mCherry* (DR 1), the *GFP* reporter was inserted into the seventh intron (right before the PTC), and *mCherry* was introduced before the canonical TAA. In DR 2, the 3× hemagglutinin (3×HA) tag was inserted into the seventh intron (right before the PTC), and the *GFP* was introduced before the canonical TAA (Supplemental Figure 9A). In both cases, the insertion of a reporter sequence into the intron caused missplicing of the intron and resulted in no detectable fluorescence of the C-terminal GFP reporter (Supplemental Figure 9B). The small intron size seems to be the main limitation in preparing a functional splicing reporter. Therefore, we needed to develop better tools to overcome this issue and successfully study the splicing events in plant systems.

We redesigned the DR strategy and prepared *pCRE1::gCRE1-1xHA/GFP* and introduced it into the *cre1-2* background (DR 3; Figure 5A). This DR 3 allows for visualization of both canonical CRE1 (GFP tagged) and CRE1^{int7} (HA tagged) proteins. Three independent lines were isolated. The presence of a GFP signal confirmed that insertion of the 1×HA tag did not affect the splicing of the seventh *CRE1* intron. To explore CRE1^{int7}-1×HA and CRE1-GFP expression, we employed immunoprecipitation (IP) on anti-HA and anti-GFP magnetic beads. We successfully immunoprecipitated monomers and multimers of CRE1^{int7}-1×HA from crude protein lysate of DR 3 line #1 (Figure 5B). The CRE1^{int7}-1×HA proteins were markedly enriched in cytokinin-treated compared to mock-treated seedlings (Figure 5B). The unbound protein fractions were further processed on anti-GFP magnetic beads, resulting in IP of CRE1-GFP homodimers (Figure 5B). The intensity of CRE1-GFP bands was comparable in mock- and BAP-treated seedlings (Figure 5B). This experiment demonstrates that *CRE1^{int7}* transcripts are translated *in planta*.

To assess the expression pattern of CRE1^{int7}, we employed immunolocalization microscopy. Using anti-HA and anti-GFP antibodies, we found that CRE1^{int7} and canonical CRE1 are co-expressed in the root stele (Figure 5D). The seedlings of *pCRE1::gCRE1^{WT}-GFP,cre1-2* were used as a control. We successfully immunolocalized CRE1-GFP protein in this control line, but only a weak background signal was observed with anti-HA antibody, confirming the specificity of the signal (Figure 5D).

Taken together, the CRE1^{int7}-GFP expressed in the Col-0 WT interferes with the signaling machinery and attenuates signal transduction, ultimately reducing cytokinin sensitivity. The expression pattern of CRE1^{int7} and canonical CRE1 receptors overlaps in root stele, and both receptors localize in the same subcellular compartments in *Arabidopsis*. Shared expression and localization patterns suggest that both receptor variants cooperate in the cytokinin signaling cascade.

DISCUSSION

Expression of a decoy receptor is a common strategy to regulate the sensing of primary pro-inflammatory cytokines and chemokines in mammals (McMahan et al., 1991). Unlike in mammalian systems, the role of decoy receptors in plant signaling cascades is not well documented. Here, we provide evidence suggesting that decoy receptors act *in planta* to regulate the signaling of the plant hormone cytokinin. We discovered that alternative splicing acts on the *Arabidopsis* cytokinin receptor gene *CRE1* and generates the *CRE1^{int7}* transcript variant. The *CRE1^{int7}* transcript retains the seventh intron, which introduces a PTC, thus encoding a truncated receptor CRE1^{int7} lacking the receiver domain essential for signal transduction (Figure 1A). We show that *CRE1^{int7}* accumulates upon cytokinin application and decreases in cytokinin biosynthesis mutants (Figure 1B and 1C), suggesting that cytokinin interferes with the plant splicing machinery to modulate the splicing of the receptor transcript.

Kinetin, a synthetic cytokinin variant, has been shown to affect alternative splicing of the human *IKBKAP* pre-mRNA, encoding

(C) The input, unbound fraction 1 (after IP α-HA), and unbound fraction 2 (after IP α-GFP) were analyzed by western blotting using α-HA and α-GFP antibodies. Mutant *cre1-2* was used as the negative control. The anticipated molecular weight (kDa) of monomer CRE1^{int7}-1×HA, multimer CRE1^{int7}-1×HA, and homodimer CRE1-GFP are shown.

(D) Immunolocalization of CRE1^{int7}-1×HA and CRE1-GFP. Four-day-old *pCRE1::gCRE1-1xHA/GFP* seedlings of three independent lines were analyzed in immunolocalization experiments using antibodies against α-HA (with Cy5-conjugated secondary antibody) and α-GFP (with Alexa Fluor 488-conjugated secondary antibody). Line *pCRE1::CRE1^{WT}-GFP* served as the positive control for CRE1-GFP detection and as the negative control for α-HA. At least 15 seedlings were analyzed per genotype. Scale bar, 20 μm.

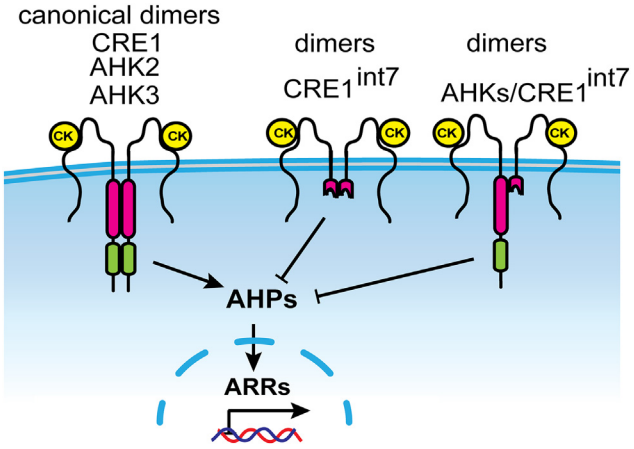

Figure 6. Mechanistic model of CRE1^{int7} action.
A cytokinin signaling pathway is executed through a histidine/aspartate phosphorelay mediated by a TCS. Active cytokinin molecules (yellow) bind to canonical AHK receptor dimers to activate them via cross-phosphorylation. The signal is then transferred to ARR transcription factors via AHPs to trigger gene expression. Alternative splicing of the *CRE1* gene produces a transcript variant, *CRE1^{int7}*, encoding a truncated receptor missing the receiver domain. CRE1^{int7} dimerizes with other CRE1^{int7} molecules or with canonical AHK monomers. In the first case, the CRE1^{int7} dimers sequester the ligands but cannot phosphorylate AHPs. In the second case, the CRE1^{int7} monomer cannot cross-phosphorylate the receiver domain of the canonical AHK monomer, as it lacks the histidine kinase domain. Vice versa, the canonical AHK monomer cannot cross-phosphorylate CRE1^{int7}, as it lacks the receiver domain. In both cases, the ligand binding results in signal attenuation.

a subunit of the Elongator complex involved in transcriptional elongation (Hims et al., 2007). A point mutation at the sixth position of the 5′ donor splice site GTAAGT in the 20th intron of the *IKBKAP* gene has been found to cause missplicing and results in the accumulation of aberrant transcripts. Consequently, decreased IKAP protein causes the human neurodegenerative disease familial dysautonomia (Hims et al., 2007). Kinetin application promoted correct intron splicing, restoring the level of IKAP protein (Hims et al., 2007). Screening of an alternatively spliced human gene collection revealed that kinetin modulates the splicing of only two other genes, *BMP2K* and *ABI2* (Hims et al., 2007). Even though the molecular mechanism underlying kinetin's effects on splicing remains unclear, its specificity indicates that cytokinin-like molecules do not interfere with the major components of the spliceosome required for constitutive splicing. Rather, they likely affect the activity of regulatory splicing factors that are specifically involved in the proper splicing of particular genes (Hims et al., 2007). Since the seventh intron is the only *CRE1* intron carrying a 5′ donor site with the GTAAGT motif (Supplemental Figures 1B and 10), we speculate that cytokinin may influence splicing through a similar conserved mechanism as in the case of the affected human *IKBKAP* intron.

Although the proportion of *CRE1^{int7}* to canonical *CRE1* mRNA transcripts is low (Supplemental Figure 1E), by employing the splicing reporter *pCRE1::gCRE1-1xHA/GFP* (DR 3), we demonstrated that *CRE1^{int7}* is translated *in planta* (Figure 5B). CRE1^{int7} co-localizes with the canonical CRE1 receptor in root stelar cells (Figure 5D). Our immunolocalization and western blot experiments showed that the relative protein expression ratio of the CRE1^{int7} variant to CRE1 is visibly stronger compared to qPCR data (Supplemental Figure 1E). A possible explanation of the discrepancy between *CRE1^{int7}* mRNA and protein levels could be increased transcript stability, efficient translation, or protein stability, leading to elevated CRE1^{int7} protein abundance. Hence, more research is needed to experimentally test these possibilities.

Some mammalian decoy receptors can outbalance the effects of the more abundant canonical receptors and attenuate the signaling cascade. A good example is the Fas decoy receptor (FDR), a member of the TNF receptor family. The molar ratio of around 0.25 of the FDR/Fas receptor (decoy/canonical receptor) was sufficient to reduce the apoptosis incidence in transfected HEK293T cells (Jenkins et al., 2000). This work demonstrates that a decoy receptor can outweigh the effects of a three times more abundant canonical receptor and inhibit the downstream signaling cascade. Similar to CRE1^{int7}, FDR is also produced by alternative splicing, resulting in loss of the C-terminal intracellular signaling death domain. The FDR is still membrane bound and still binds the ligand but cannot activate the downstream signaling cascade. As a result, FDR competes for ligand binding with its canonical counterpart, Fas receptor (Felix and Savvides, 2017).

Our findings suggest two modes of CRE1^{int7}cytokinin signaling modulation (Figure 6). The first is by dimerization with canonical receptors, preventing their activation via cross-phosphorylation. The heterodimerization of CRE1^{int7} with AHK2 and AHK3, the only active cytokinin receptors in the *cre1-2* mutant, could be the reason for a dwarfed phenotype of CRE1^{int7}/*cre1-2* homozygotes. Second, CRE1^{int7} multimers compete with canonical receptors for ligand binding and sequester them. Both mechanisms are not contradictory but may act in concert in plant tissues.

Although the decoy receptor phenomenon has not yet been described in plant hormonal pathways, we can find some analogical fine-tuning mechanisms in plant hormone pathways acting downstream of the receptors. These mechanisms involve the intron retention transcripts encoding truncated proteins, often impeding the function of the full-length proteins to modulate the signal pathway. Such a mechanism was described for jasmonate and abscisic acid signaling. *JAZ* genes, which encode transcription factors of jasmonic acid signaling, undergo intron retention, producing truncated proteins that attenuate this pathway (Chung et al., 2010). A similar mechanism in the abscisic acid signaling pathway can be observed where intron retention occurs in the *HAB1* gene, encoding a regulatory phosphatase (Wang et al., 2015). This process results in the formation of a truncated protein lacking the phosphatase activity. Typically, the canonical HAB1 interacts with the effector kinase SnRK2.6/OST1 to inhibit its activity and the downstream signaling cascade. However, the truncated HAB1 variant retains its ability to interact with SnRK2.6/OST1 but can no longer inhibit its activity (Wang et al., 2015). Therefore, alternative splicing of the *HAB1* gene represents a sophisticated mechanism that regulates abscisic acid signaling in response to external stimuli (Wang et al., 2015).

Taken together, here we identified a previously unknown regulatory mechanism of the cytokinin signaling pathway mediated by

intron retention in transcripts of the cytokinin receptor gene *CRE1*. We showed that CRE1^{int7}, acting as the decoy receptor, provides competitive inhibition to other canonical cytokinin receptors and thus attenuates the signaling cascade (Figure 6). Since cytokinin increases *CRE1^{int7}* abundance (Figure 1B), we propose that CRE1^{int7} provides a so far overlooked feedback mechanism fine-tuning cytokinin-regulated plant development and acting as the gatekeeper in situations when the cytokinin level increases.

METHODS

Plant materials and growth conditions

All mutants used in the study were Col-0 ecotypes that served as a WT control. *cre1-2*, *ipt2/9*, and *ipt3/5/7* mutants were provided by Dr. Tatsuo Kakimoto (Osaka University, Japan). *upf1-5* and *upf3-1* were provided by Dr. Nicola Cavallari (Institute of Science and Technology Austria).

The seeds were surface sterilized and sown on standard MS medium (0.43% MS medium, 1% sucrose, and 1% plant agar, from Duchefa, catalog number P1001) plates and stratified at 4°C in the dark for 2–3 days. Seedlings were then grown on vertically oriented plates in a growth chamber at 21°C under long-day conditions (16 h light of 120 μmol m^{-2} s^{-1}/8 h dark).

Cloning and construct preparation

The sequences of all primers used in this work are listed in Supplemental Table 1. For bacterial assays in *E. coli*, the original *pIN-III* expression vector was first modified by inserting a *4xMyc* tag sequence followed by a *tNOS* terminator. The resulting construct was named *pIN-III_4xMyc_tNOS*. ORFs of *CRE1* (primers: CRE1_ATG1_Fw_BamHI and CRE1_WT_rev_SpeI) and *CRE1^{int7}* (primers: CRE1_ATG1_Fw_BamHI and CRE1int7_rev_SpeI) were PCR amplified from *A. thaliana* Col-0 root cDNA and cloned into *pIN-III_4xMyc_tNOS* under *Bam*HI and *Spe*I restriction sites.

To generate constructs for transient expression in protoplasts and the *TCS::LUC* assay, the *EGFP* reporter gene was subcloned (primers: EGFP_Fw_EagI and GFP_rev_EagI_XhoI_EcoRV_XbaI) into the *pENTR2B* vector using the *Eag*I restriction enzyme. The resulting construct, *pENTR2B_GFP*, has a unique *Not*I site located upstream of the *EGFP* ORF. The *CRE1* (primers: F1 and R1) and *CRE1^{int7}* (primers: F1 and CRE1bint7_R_NotI) ORFs were PCR amplified and cloned into *pENTR2B_GFP* under *Sal*I and *Not*I restriction sites to allow for C-terminal fusion with *EGFP*. The *CRE1-GFP* and *CRE1^{int7}-GFP* fusions were shuttled into the *p2GW7,0* expression vector using a Gateway LR reaction to generate the *CaMV35S::CRE1-GFP* and *CaMV35S::CRE1^{int7}-GFP* constructs.

The ER marker construct *35S::AtWAK2-tdTomato-HDEL* was provided by Dirk Becker (University of Hamburg, Hamburg, Germany).

The *pENTR2B::CRE1/AHK4-EGFP* construct containing a genomic fragment of *CRE1* fused with an *EGFP* reporter (Kubiasová et al., 2020) was used to generate *pCRE1::CRE1-GFP*. The *TMVΩ* translational enhancer sequence was introduced upstream of the first *CRE1* ATG using the oligo annealing method (TMV_oligo_F_SalI; TMV_oligo_R_SalI) into the *Sal*I restriction site. The resulting construct, *pENTR2B::TMVΩ_gCRE1-EGFP*, served as a template for preparing the *pENTR2B::TMVΩ_gCRE1^{int7}-EGFP* construct by inversion PCR method to remove the region downstream of the PTC in intron 7 of the *CRE1* gene. The phosphorylated primers gCRE1_int7_Rv and Linker_fw were used. The PCR product was treated with *Dpn*I enzyme to remove the template plasmid, gel purified using NucleoSpin Gel and PCR Clean-up Kit (Macherey-Nagel), and circularized using T4 DNA ligase.

Since the original GFP-only control construct did not show any fluorescence *in planta*, the first *CRE1* exon and intron sequences and the beginning of the second exon were included. The control GFP-only construct was generated by inversion PCR on *pENTR2B::TMVΩ_gCRE1-EGFP* (primers: GFP_GA2_FW; pEN_GFP_CTRL_GA_RV) to skip the region between the second and last exons of the *CRE1* gene. The PCR product was treated with the *Dpn*I enzyme to remove the template plasmid, gel purified, and self-assembled using Gibson assembly (NEBuilder HiFi DNA Assembly Master Mix, New England Biolabs [NEB]).

All resulting *pENTR2B* constructs were verified by sequencing, shuttled into the *pWOL::GW* vector (Michniewicz et al., 2015) carrying the 2 kbp promoter region of the *WOL/CRE1/AHK4* gene (At2g01830) using a Gateway LR reaction (Thermo Fisher Scientific), and sequenced.

The full native construct *pCRE1::CRE1^{WT}-GFP* and deletion construct *pCRE1::CRE1$^{\Delta int7}$-GFP* were cloned as follows. The construct *pENTR2B::TMVΩ_gCRE1-EGFP* served as the starter material for cloning. First, the construct was opened using *Sal*I and *Hpa*I restriction enzymes.

The *CRE1* promoter region (−3953 bp) was PCR amplified from *Arabidopsis* genomic DNA (pCRE1_F1224_SalI; CRE1_exon2_R3099) up to the second exon. The PCR product was purified and digested using *Sal*I and *Hpa*I (naturally occurring in the first intron). The fragment containing the promoter region was ligated into the linearized *pENTR2B::TMVΩ_gCRE1-EGFP.*

Next, the resulting clone was digested with *Xba*I downstream of the *GFP* reporter to accommodate the terminator sequence. The terminator region (2607 bp) downstream of the *CRE1* gene was PCR amplified from *Arabidopsis* genomic DNA using primers (tCRE1_F_NheI_AscI; tCRE1_R11011_NheI), purified, and digested using *Nhe*I. The fragment was cloned into the *Nhe*I-linearized plasmid. The presence and correct orientation of the terminator region were verified using colony PCR and sequencing. The final entry clone, *pENTR2B::pCRE1::gCRE1^{WT}-EGFP_tCRE1*, therefore contains a complete seamless genomic *CRE1* locus consisting of an ~4 kbp promoter, *CRE1* gene, and *GFP* reporter followed by an ~2.6 kbp terminator region.

Since the entry clone was too large for the subsequent genetic manipulations (e.g., intron deletion), we decided to first subclone the 4485-bp-long fragment of the *CRE1* locus by cutting it out from *pEN::pCRE1::gCRE1^{WT}-GFP_tCRE1* using the *Hpa*I enzyme and ligating into the *pJET1.2* blunt vector (Thermo Fisher Scientific). Here, the region of the seventh intron was removed using inversion PCR using primers delINT7_GA_rev and delINT7_GA_fw. The PCR product was treated with the *Dpn*I enzyme to remove the template plasmid, gel purified, and self-assembled using Gibson assembly (NEBuilder HiFi DNA Assembly Master Mix, NEB). The resulting clone was verified by sequencing, and the corresponding *CRE1 Δint7* locus (lacking the seventh intron) was PCR amplified using primers gCRE1_GA_Fw and gCRE1_GA_rev, gel purified, digested using *Hpa*I, and shuffled back into the *Hpa*I-digested *pEN::pCRE1::gCRE1^{WT}-GFP_tCRE1*. The resulting construct, *pEN::pCRE1::CRE1$^{\Delta int7}$-GFP_tCRE1*, was verified by sequencing.

The control vector *pEN::pCRE1::GFP_tCRE1*, expressing free GFP, was prepared using a similar design as for the TMVΩ-containing constructs. Here, the promoter is seamlessly followed by the first *CRE1* exon, the first intron, and the beginning of the second exon and fused with the *GFP* reporter. This construct was prepared by inversion PCR (pEN_GFP_CTRL_GA_FW; pEN_GFP_CTRL_GA_RV) on the template *pEN::pCRE1::gCRE1^{WT}-GFP_tCRE1*, followed by Gibson assembly to self-circularize the construct.

The resulting entry clones were shuffled into the *pMCS::GW* vector (Michniewicz et al., 2015) using a Gateway LR reaction (Thermo Fisher

Scientific), and the resulting binary constructs were verified by sequencing.

DRs 1–3 were prepared as follows. The starting point for DR 1 was *pENTR2B::TMVΩ_gCRE1int7-EGFP.* The PCR product containing the *mCherry* sequence was amplified from pDONR221_mCherry, available in the lab (primers mCherry_F_XhoI and mCherry_R_XbaI), and cloned into *pENTR2B::TMVΩ_gCRE1int7-EGFP* using *Xho*I and *Xba*I sites. The C-terminal region of the *CRE1* gene was PCR amplified from *Arabidopsis* genomic DNA using primers EGFP_F_AvaII and gCRE1_R_SalI. The PCR product was digested by *Ava*II and *Sal*I enzymes, while the interstep cloning vector was opened using *Ava*II and *Xho*I. *Sal*I sites are compatible with *Xho*I. The resulting entry clone *pENTR::TMV_gCRE1int7-GFP-mCherry* thus contained a genomic *CRE1* sequence with a *GFP* reporter introduced into the seventh intron (right before PTC) and *mCherry* reporter inserted before the canonical termination codon TAA. The cassette was then shuttled into the *pWOL::GW* vector and used for plant transformation.

The starting point for DRs 2 and 3 was the *pJET1.2::gCRE1_HpaI* vector containing the *Hpa*I fragment of the *CRE1* genomic locus. The 3×HA tag was PCR amplified from pEN_B2 using primers 3×HA_F4 and 3×HA_R4. The 1×HA tag was synthesized as a long oligo (1×HA_oligo_R). Both fragments were introduced into *pJET1.2::gCRE1_HpaI* by Gibson assembly. The backbone was amplified by primers bckb_F3_4 and bckb_R3_4. The resulting cassette was PCR amplified using gCRE1_GA_Fw and gCRE1_GA_rev primers and subcloned into the *Hpa*I-digested *pENTR2B::gCRE1-GFP* vector by Gibson assembly. The resulting entry clones thus contained a 4.5-kbp-long promoter followed by a *CRE1* genomic sequence. The *3×HA* (DR 2) or *1×HA* tag (DR 3) was inserted into the seventh intron (right before the PTC), and the *GFP* reporter was introduced before the canonical termination codon, followed by a 2.5-kbp-long terminator. The cassettes were subcloned in the *pMCS::GW* using a Gateway LR reaction and used for plant transformation.

The constructs for BiFC were prepared as follows. First, the ORFs of *CRE1^{int7}*, *CRE1*, *AHK2*, and *AHK3* were PCR amplified from *Arabidopsis* cDNA without the STOP codon. The *AHK2*-containing PCR product (AHK2_Fw_BamHI_KOZAK; AHK2_R_NotI) was cloned into *pENTR2B* under *Bam*HI and *Not*I restriction sites. The other three genes were introduced into the *pENTR2B* vector by Gibson assembly. The plasmid backbone was PCR amplified from the *pENTR2B* plasmid using primers pDONR221_R and pDONR221_F and gel purified. The PCR products containing *CRE1^{int7}* (CRE1B_F1; CRE1int7_SD_mut_R), *CRE1* (CRE1B_F1; CRE1_R1), and *AHK3* (AHK3_F1, AHK3_R1) were gel purified and assembled with the pENTR2B backbone using NEBuilder HiFi DNA Assembly Master Mix (NEB). The expression constructs for BiFC were prepared by a two-fragment LR reaction. Here, the cDNA-containing entry clones were fused with N- or C-terminal mNeonGreen fragments carried by the *pJET_C1* or *pJET_C3* vector and introduced into the expression vector *pJET1.2_35S_DZ_R1-R3_t35S*. This Gateway-compatible set of BiFC vectors was prepared in this work; for details, see the supplemental information.

The resulting expression clones were sequenced. During the cloning process, we encountered serious issues with negative selection in *E. coli*, yielding clones with mutations in the cytokinin receptor genes (especially in *AHK2* and *AHK3*) and very low plasmid yield. This problem was solved by using a special *E. coli* strain, CopyCutter EPI400 Competent Cells (Biozym Scientific), allowing for inducible plasmid propagation.

The *FLS2* (coding sequence) was cloned into *pDONR221* by BP reaction (Gateway Cloning, Thermo Fisher Scientific), and the resulting entry clone (provided by Caterina Giannini, Institute of Science and Technology Austria Austria) was further shuttled into *pB7MWG2* via LR reaction (Gateway Cloning, Thermo Fisher Scientific). The final expression construct was used for FRET/FLIM.

All plasmid constructs prepared in this work are listed in Supplemental Table 2.

Plant transformation

Transgenic *Arabidopsis* plants were generated by the floral dip method (Clough and Bent, 1998) using *Agrobacterium tumefaciens* strain GV3101. Transformed T1 seedlings were selected in soil by spraying with 0.02% BASTA solution (glufosinate-ammonium, Bayer). The following transgenic generations were selected on MS medium supplemented with 15 μg ml^{-1} phosphinothricin.

Genotyping

Genotyping of the *cre1-2* allele in *pCRE1::CRE1^{int7}-GFP* crossed with *cre1-2* was challenging because the genomic *CRE1* locus is the same as the *pCRE1::CRE1^{int7}-GFP* cassette. Therefore, the standard primer set could not be used, as it anneals to both regions. The *cre1-2* transfer DNA is inserted at the beginning of the second exon (Supplemental Figure 10). Due to this similarity, any forward primer designed (located upstream of transfer DNA) always anneals to both regions. The only way to overcome this issue was to design reverse primer annealing downstream of the seventh intron, as this region is absent in the *pCRE1::CRE1^{int7}-GFP* cassette. As a result, the amplicon for the WT allele is rather long (2486 bp), which is not optimal for genotyping. Together with the competitive binding of the forward primer and long amplicon, the WT bands are sometimes faint but still clearly distinguishable. The WT allele was genotyped using primers AHK4_ATG4_Fw and CRE1_R554. The mutant *cre1-2* allele was genotyped using F_5346 and pPCVICEn3596.

RT-qPCR

Total RNA was extracted from roots of 4-day-old untreated seedlings (Figure 1C and 1D) and roots of seedlings sprayed with mock solvent (DMSO, dimethyl sulfoxide) or 1 μM BAP for 60 min (Figure 1B). As shown in Supplemental Figure 4, total RNA was extracted from whole seedlings submerged in $^1/_2$ MS medium supplemented with DMSO solvent (mock), 10 nM BAP, or 1μM BAP for 120 min. In all cases, RNA was extracted using the RNAqueous Total RNA Isolation Kit (Thermo Fisher Scientific).

RNA was treated twice with TURBO DNase (Thermo Fisher Scientific). The presence of genomic DNA contamination was tested with the primer pair specifically annealing in the promoter region of the cytokinin-unrelated gene *ERF8* (primers ERF8_TPF; ERF8_TPR; Supplemental Figure 1D).

Poly(dT) cDNA was prepared from 3 μg total RNA with RevertAid H Minus Reverse Transcriptase (Thermo Fisher Scientific) and analyzed on the StepOnePlus Real-Time PCR System (Life Technologies) with gb SG PCR Master Mix (Generi Biotech) according to the manufacturer's instructions. The expression of all *CRE1* transcripts was quantified using a primer pair specific to the last *CRE1* exon (F3 and R3). The *CRE1^{int7}* transcripts were quantified using a primer pair annealing to exon 7 and intron 7 (F2 and R2). *ARR5*, *ARR7*, and *ARR16* expression was quantified using primer pairs (ARR5_fw and ARR5_rev; ARR7_fw and ARR7_rev; ARR16_fw and ARR16_rev). The relative expression of the respective targets was normalized to the housekeeping gene *TUB3* (TUB3_F2426 and TUB3_R2616) or *PP2A* (PP2A_fw and PP2A_rev). The proportion of the seventh *CRE1* intron was calculated as *CRE1^{int7}* expression normalized to all *CRE1* transcripts (F3 and R3). The primer position within the *CRE1* transcript is shown in Figure 1A and Supplemental Figure 1B. For cytokinin treatment experiments, the fold change refers to mock treatment. In the case of the mutant experiment with *ipt* and *upf* mutants as well as with *pCRE1::CRE1^{int7}-GFP* line #1, the fold change refers to the Col-0 WT. Absolute quantification of *CRE1* and *CRE1^{int7}* was performed using the calibration curve of diluted *pENTR2B::gCRE1* containing the *CRE1* genomic sequence.

Plant material for cytokinin treatment (Figure 1B) was prepared and harvested on separate days in a total of nine independent experiments.

RT-qPCR data were collected from five technical replicates. In the case of *ipt*, *upf* mutants (Figure 1C and 1D), and the *pCRE1::CRE1^{int7}-GFP* line (Supplemental Figure 4), four to five biological replicates were used, each with three technical replicates.

Microscopy

Carl Zeiss LSM800 and LSM900 confocal scanning microscopes equipped with a 40× Plan-Apochromat water immersion objective were employed to follow the expression of the fluorescent reporters. Images were captured using excitation wavelengths of 488 nm for EGFP and Alexa Fluor 488 and 561 nm for tdTomato, Cy5, and propidium iodide. Carl Zeiss Zen Blue and ImageJ v.1.53c were used for image post-processing.

Ligand binding assay in *E. coli*

The receptor binding assay (Romanov et al., 2005) was performed using the *E. coli* strain KMI001 clones carrying the *pIN-III_4xMyc_tNOS* constructs expressing 4×Myc-tagged *CRE1* or *CRE1^{int7}*. The expression of CRE1 proteins was induced with 0.25 mM isopropyl β-D-1-thiogalactopyranoside in cultures of optical density 600 (OD_{600}) (0.6–0.7) and then cultivated for 5 h at 18°C. The competitive binding assay was performed as described previously (Kubiasová et al., 2020). The competition reaction was allowed to proceed with 3 nM [2-^{3}H]*t*Z and 10 μM unlabeled iP and *t*Z or 0.1% (v/v) DMSO (solvent, mock control). [2-^{3}H]*t*Z was provided by Dr. Zahajská from the Isotope Laboratory, Institute of Experimental Botany of the Czech Academy of Sciences. The statistical significance was evaluated with Student's *t*-test.

Receptor activation assay in *E. coli*

The receptor activation assay was performed as described previously (Suzuki et al., 2001). The identical *pIN-III* clones of *E. coli* strain KMI001 used in the ligand-binding assay were also used for this assay. The expression of CRE1 proteins was induced with 0.25 mM isopropyl β-D-1-thiogalactopyranoside in cultures of OD_{600} (0.6–0.7) and then cultivated for 16 h at 18°C. The induced culture was diluted to OD_{600} (0.2), and the experiment was performed in 96-well plates for 6 h at 18°C in M9 medium containing 1 μM iP or DMSO (mock). The statistical significance was evaluated with Student's *t*-test.

Transient expression in protoplasts and *TCS::LUC* assay

The transient expression was performed in protoplasts isolated from a 4-day-old *Arabidopsis* Col-0 root suspension culture. Protoplasts were transfected by polyethylene glycol as described previously (Hurný et al., 2020). The quality of protoplasts was checked under the microscope, and density was quantified by spectrophotometry (OD_{600}). Protoplasts were diluted in B5 glucose-mannitol solution to 1.6 OD_{600}, corresponding to 10^5 cells. 50 μl of protoplasts was co-transfected with 2 μg of ER marker (*35S::AtWAK2-tdTomato-HDEL*) and 5 μg of *p2GW7.0* plasmid DNA (*CaMV35S::CRE1-GFP*, *CaMV35S::CRE1^{int7}-GFP*, or *CaMV35S::GFP*). The transient expression of GFP fusion proteins was allowed for 16 h after polyethylene glycol transfection in the dark at room temperature. Transfected protoplasts were mounted on Nunc glass-bottom dishes (Thermo Fisher Scientific, catalog number 150680) and observed with a Carl Zeiss LSM 800 laser-scanning confocal microscope.

The expression of CRE1-GFP proteins was verified by western blotting with an anti-GFP antibody on microsomal fractions isolated from protoplasts according to the protocol described previously (Hajný et al., 2020). In the case of protoplasts expressing the free GFP, the protein was precipitated from the soluble protein fraction by methanol/chloroform procedure. Briefly, a mixture of 200 μl of chloroform, 800 μl methanol, and 600 μl of Milli-Q water was added to 200 μl of the soluble protein fraction, vortexed, and centrifuged at 13 000 rpm at room temperature for 1 min. The upper phase was discarded, and 600 μl of fresh methanol was added to the mixture, vortexed, and centrifuged for 3 min. The supernatant was discarded. The dried pellet was resuspended in 50 μl of protein extraction buffer (50 mM Tris, 150 mM NaCl, 0.5 mM EDTA, PhosSTOP, cOmplete, and EDTA-free protease inhibitor cocktail) with detergents (0.5% Triton X-100, 0.5% 3-[(3-Cholamidopropyl)dimethylammonio]-1-propanesulfonate) and analyzed on SDS–PAGE.

The luciferase transient expression assay (*TCS::LUC*) was performed on protoplasts isolated from 4-day-old *Arabidopsis* Col-0 root suspension culture as described previously (Kubiasová et al., 2020). Protoplasts were co-transfected with 2.5 μg of *TCS::LUC*, a cytokinin reporter plasmid (Müller and Sheen, 2008) expressing firefly luciferase, 2.5 μg of normalization plasmid containing *Renilla* luciferase, and 5 μg of *p2GW7,0* plasmid carrying either cytokinin receptor (*CaMV35S::CRE1-GFP* and *CaMV35S::CRE1^{int7}-GFP*) or GFP only (*CaMV35S::GFP*) constructs. The statistical significance was evaluated using Student's *t*-test.

BiFC and FRET-FLIM

BiFC and FRET-FLIM imaging were done in *Arabidopsis* protoplasts isolated from root cell suspension culture Col-0. Protoplast transfection was performed as described above.

Imaging of BiFC and FRET-FLIM experiments was done using a Leica SP8 with a FALCON FLIM detector (mNeonGreen/GFP, excitation 488 nm with detection length of 493–582 nm; mCherry, excitation 587 nm with detection length of 592–779 nm), and the lifetime was measured using LAS X software (FLIM).

Western blotting

For immunoblot analysis, 20 μl of microsomal protein fractions (*CaMV35S::CRE1-GFP* and *CaMV35S::CRE1^{int7}-GFP*) or soluble protein fractions (for *CaMV35S::GFP*) isolated from transfected protoplasts were separated by SDS–PAGE (under non-reducing conditions without 2-mercaptoethanol) and subjected to immunoblotting using an anti-GFP-HRP antibody (130-091-833, Miltenyi Biotec, dilution 1:5000).

In the case of expression in *E. coli*, the bacterial pellet was resuspended in 1× Laemmli buffer with 2% 2-mercaptoethanol, boiled at 95°C for 5 min, and centrifuged at 14 000 rpm. 5 μl of supernatant was analyzed by SDS–PAGE and subjected to immunoblot analysis with mouse anti-Myc (clone 4a6, Millipore, catalog number 05-724, dilution 1:1000) and goat anti-mouse immunoglobulin G-horseradish peroxidase (HRP) (Santa Cruz Biotechnology, catalog number sc-2005, dilution 1:5000).

IP

Plant material (0.2 g) was ground in liquid nitrogen and added to 1 ml of lysis buffer (50 mM Tris–HCl [pH 7.4], 150 mM NaCl, 1 mM EDTA, 1% Triton X-100 with 20 μl cOmplete EDTA-free protease inhibitor cocktail (Roche) and extracted for 60 min on ice with occasional mixing. Debris was pelleted by centrifugation at 20 500 *g* for 2 × 20 min. The supernatant was retained, and another 20 μl of protease inhibitor cocktail was added. A 100 μl aliquot was kept for further analysis (input). The rest of the extract was incubated with 50 μl anti-HA magnetic bead agarose (Thermo) for 2 h on a rotator in the fridge. The agarose beads were separated on a magnet and washed four times with lysis buffer. A 100 μl aliquot was kept for further analysis (unbound fraction 1). The remaining unbound fraction 1 was further mixed with 50 μl of GFP-Trap magnetic agarose beads (Chromotek) for 2 h on a rotator in the fridge. The agarose beads were separated on a magnet and washed four times with lysis buffer. A 100 μl aliquot was kept for further analysis (unbound fraction 2).

The anti-HA and GFP-Trap beads were incubated at 95°C for 5 min in 100 μl 1× Laemmli buffer without 2-mercaptoethanol (Bio-Rad). Samples were separated on 7% SDS–PAGE gels, blotted onto a Immobilon-P membrane, and probed with HRP-conjugated anti-HA antibody (1:1000,

Thermo Fisher Scientific) or HRP-conjugated anti-GFP antibody (1:1000, Miltenyi) and visualized by chemiluminescence.

Immunolocalization

Immunolabeling in roots (4- to 5-day-old seedlings) was done using an automated system (Intavis *in situ* pro) according to a published protocol (Sauer et al., 2006). Roots were fixed in 4% paraformaldehyde for 1 h in a vacuum at room temperature. Afterward, seedlings were incubated for 30–45 min in PBS (2.7 mM KCl, 137 mM NaCl, 4.3 mM Na_2HPO_4 $2H_2O$, and 1.47 mM KH_2PO_4 [pH 7.4]) containing 2% Driselase (Sigma) and then in PBS supplemented with 3% NP40 and 20% DMSO. After blocking with 3% BSA in PBS, samples were incubated with primary antibody for 2 h. Antibody dilutions were rat monoclonal anti-GFP, clone 1A5 (Agrisera, 1:500) and mouse monoclonal anti-HA (Thermo Fisher Scientific, 1:500). Secondary antibody incubation was carried out for 2 h. Goat anti-rat Alexa Fluor 488 (Thermo Fisher Scientific) and Cy5-conjugated anti-mouse (Thermo Fisher Scientific) were diluted 1:600 in the blocking solution. Samples were mounted in a solution containing 25 mg ml^{-1} 1,4-Diazabicyclo[2.2.2]octane solution (Sigma) in 90% glycerol, 10% PBS (pH 8.5). The signal was monitored using a confocal laser-scanning microscope (LSM 900, Carl Zeiss). Images were analyzed by using ImageJ v.1.53g.

Root phenotypes

Root growth and LR number were assayed using seedlings grown vertically on standard MS medium. Seedlings were grown on MS medium for 3 days, transferred to new MS plates supplemented with 20 nM BAP or DMSO (mock control), and grown for another 10 days. Images were taken with an EPSON Perfection v,800 photo scanner at selected time points. The root length was evaluated 9 days after transfer ($n \geq 11$). LR quantification was performed 11–14 days after transfer ($n \geq 13$). The statistical significance between groups was evaluated with non-parametric Kruskal–Wallis ANOVA followed by multiple comparisons of mean ranks. All results represent the mean value ± standard deviation.

Statistical analysis

The statistical significance was evaluated with Student's *t*-test or parametric one-way ANOVA to compare the differences between groups, followed by Tukey's multiple-comparisons test for post hoc analysis ($p < 0.05$).

FUNDING

This work was supported by the Czech Science Foundation via project 23-07363S (to D.Z., J.H., K.V., and O.N.). This research was further supported by the Scientific Service Units (SSU) of ISTA through resources provided by the Imaging and Optics Facility and the Life Science Facility.

ACKNOWLEDGMENTS

We dedicate this paper to the deceased Petr Galuszka for his inspiration and support of our project. We thank Prof. Peter Hedden for constructive criticism of the manuscript and English editing. No conflict of interest is declared.

AUTHOR CONTRIBUTIONS

Y.I., E.B., and D.Z. initiated the project and designed the experiments. I.K., Y.I., K.V., and D.Z. conducted RT-qPCR. K.K. performed the ligand-binding and receptor activation assay. J.H. and D.Z. performed microscopy experiments. J.F. and Z.G. provided the material and performed BiFC and FRET/FLIM. M.G. edited figures. H.S. and D.Z. conducted protoplast experiments. M. Králová and K.V. performed most of the *Arabidopsis* work and phenotyping. A.K. performed WB and IP experiments. A.M. performed immuno-microscopy. M.H. and K.V. performed statistic analyses. M. Kovačik performed bioinformatic analyses. E.B., J.F., O.N., and D.Z. acquired funding. I.K., J.H., E.B., and D.Z. wrote the manuscript. All authors discussed and commented on the manuscript.

SUPPLEMENTAL INFORMATION

Supplemental information is available at *Molecular Plant Online*.

Received: July 18, 2023
Revised: June 27, 2024
Accepted: November 3, 2024
Published: November 5, 2024

REFERENCES

Antoniadi, I., Novák, O., Gelová, Z., Johnson, A., Plíhal, O., Simerský, R., Mik, V., Vain, T., Mateo-Bonmatí, E., Karady, M., et al. (2020). Cell-surface receptors enable perception of extracellular cytokinins. Nat. Commun. **11**:4284.

Arciga-Reyes, L., Wootton, L., Kieffer, M., and Davies, B. (2006). UPF1 is required for nonsense-mediated mRNA decay (NMD) and RNAi in Arabidopsis. Plant J. **47**:480–489.

Ashkenazi, A. (2002). Targeting death and decoy receptors of the tumour-necrosis factor superfamily. Nat. Rev. Cancer **2**:420–430.

Auer, C.A. (1996). Cytokinin inhibition of Arabidopsis root growth: An examination of genotype, cytokinin activity, and N6-benzyladenine metabolism. J. Plant Growth Regul. **15**:201–206.

Bar, M., Sharfman, M., Ron, M., and Avni, A. (2010). BAK1 is required for the attenuation of ethylene-inducing xylanase (Eix)-induced defense responses by the decoy receptor LeEix1. Plant J. **63**:791–800.

Brandstatter, I., and Kieber, J.J. (1998). Two Genes with Similarity to Bacterial Response Regulators Are Rapidly and Specifically Induced by Cytokinin in Arabidopsis. Plant Cell **10**:1009–1019.

Caesar, K., Thamm, A.M.K., Witthöft, J., Elgass, K., Huppenberger, P., Grefen, C., Horak, J., and Harter, K. (2011). Evidence for the localization of the Arabidopsis cytokinin receptors AHK3 and AHK4 in the endoplasmic reticulum. J. Exp. Bot. **62**:5571–5580.

Chung, H.S., Cooke, T.F., DePew, C.L., Patel, L.C., Ogawa, N., Kobayashi, Y., and Howe, G.A. (2010). Alternative splicing expands the repertoire of dominant JAZ repressors of jasmonate signaling: Alternative splicing of Arabidopsis JAZ genes. Plant J. **63**:613–622.

Clough, S.J., and Bent, A.F. (1998). Floral dip: a simplified method for Agrobacterium -mediated transformation of Arabidopsis thaliana. Plant J. **16**:735–743.

Felix, J., and Savvides, S.N. (2017). Mechanisms of immunomodulation by mammalian and viral decoy receptors: insights from structures. Nat. Rev. Immunol. **17**:112–129.

Feng, J., Wang, C., Chen, Q., Chen, H., Ren, B., Li, X., and Zuo, J. (2013). S-nitrosylation of phosphotransfer proteins represses cytokinin signaling. Nat. Commun. **4**:1529.

Ferrell, J.E. (2013). Feedback loops and reciprocal regulation: recurring motifs in the systems biology of the cell cycle. Curr. Opin. Cell Biol. **25**:676–686.

Gomord, V., Denmat, L.-A., Fitchette-Lainé, A.-C., Satiat-Jeunemaitre, B., Hawes, C., and Faye, L. (1997). The C-terminal HDEL sequence is sufficient for retention of secretory proteins in the endoplasmic reticulum (ER) but promotes vacuolar targeting of proteins that escape the ER. Plant J. **11**:313–325.

Gordon, S.P., Chickarmane, V.S., Ohno, C., and Meyerowitz, E.M. (2009). Multiple feedback loops through cytokinin signaling control stem cell number within the *Arabidopsis* shoot meristem. Proc. Natl. Acad. Sci. USA **106**:16529–16534.

Hajný, J., Prát, T., Rydza, N., Rodriguez, L., Tan, S., Verstraeten, I., Domjan, D., Mazur, E., Smakowska-Luzan, E., Smet, W., et al. (2020). Receptor kinase module targets PIN-dependent auxin transport during canalization. Science **370**:550–557.

He, Z.-H., Cheeseman, I., He, D., and Kohorn, B.D. (1999). A cluster of five cell wall-associated receptor kinase genes, Wak1–5, are expressed in specific organs of Arabidopsis. Plant Mol. Biol. **39**:1189–1196.

Higuchi, M., Pischke, M.S., Mähönen, A.P., Miyawaki, K., Hashimoto, Y., Seki, M., Kobayashi, M., Shinozaki, K., Kato, T., Tabata, S., et al. (2004). *In planta* functions of the *Arabidopsis* cytokinin receptor family. Proc. Natl. Acad. Sci. USA **101**:8821–8826.

Hims, M.M., Ibrahim, E.C., Leyne, M., Mull, J., Liu, L., Lazaro, C., Shetty, R.S., Gill, S., Gusella, J.F., Reed, R., and Slaugenhaupt, S.A. (2007). Therapeutic potential and mechanism of kinetin as a treatment for the human splicing disease familial dysautonomia. J. Mol. Med. **85**:149–161.

Hosoda, K., Imamura, A., Katoh, E., Hatta, T., Tachiki, M., Yamada, H., Mizuno, T., and Yamazaki, T. (2002). Molecular Structure of the GARP Family of Plant Myb-Related DNA Binding Motifs of the Arabidopsis Response Regulators. Plant Cell **14**:2015–2029.

Hurný, A., Cuesta, C., Cavallari, N., Ötvös, K., Duclercq, J., Dokládal, L., Montesinos, J.C., Gallemí, M., Semerádová, H., Rauter, T., et al. (2020). SYNERGISTIC ON AUXIN AND CYTOKININ 1 positively regulates growth and attenuates soil pathogen resistance. Nat. Commun. **11**:2170.

Inoue, T., Higuchi, M., Hashimoto, Y., Seki, M., Kobayashi, M., Kato, T., Tabata, S., Shinozaki, K., and Kakimoto, T. (2001). Identification of CRE1 as a cytokinin receptor from Arabidopsis. Nature **409**:1060–1063.

Jenkins, M., Keir, M., and McCune, J.M. (2000). A membrane-bound Fas decoy receptor expressed by human thymocytes. J. Biol. Chem. **275**:7988–7993.

Kashkan, I., Hrtyan, M., Retzer, K., Humpolíčková, J., Jayasree, A., Filepová, R., Vondráková, Z., Simon, S., Rombaut, D., Jacobs, T.B., et al. (2022). Mutually opposing activity of PIN7 splicing isoforms is required for auxin-mediated tropic responses in Arabidopsis thaliana. New Phytol. **233**:329–343.

Kim, H.J., Chiang, Y.-H., Kieber, J.J., and Schaller, G.E. (2013). SCF ^{KMD} controls cytokinin signaling by regulating the degradation of type-B response regulators. Proc. Natl. Acad. Sci. USA **110**:10028–10033.

Kubiasová, K., Montesinos, J.C., Šamajová, O., Nisler, J., Mik, V., Semerádová, H., Plíhalová, L., Novák, O., Marhavý, P., Cavallari, N., et al. (2020). Cytokinin fluoroprobe reveals multiple sites of cytokinin perception at plasma membrane and endoplasmic reticulum. Nat. Commun. **11**:4285.

Lemmon, M.A., Freed, D.M., Schlessinger, J., and Kiyatkin, A. (2016). The Dark Side of Cell Signaling: Positive Roles for Negative Regulators. Cell **164**:1172–1184.

Lohrman, J. (2001). The response regulator ARR2: a pollen-specific transcription factor involved in the expression of nuclear genes for components of mitochondrial Complex I in Arabidopsis. Mol. Genet. Genom. **265**:2–13.

Lomin, S.N., Myakushina, Y.A., Arkhipov, D.V., Leonova, O.G., Popenko, V.I., Schmülling, T., and Romanov, G.A. (2018). Studies of cytokinin receptor–phosphotransmitter interaction provide evidences for the initiation of cytokinin signalling in the endoplasmic reticulum. Funct. Plant Biol. **45**:192–202.

Mähönen, A.P., Bonke, M., Kauppinen, L., Riikonen, M., Benfey, P.N., and Helariutta, Y. (2000). A novel two-component hybrid molecule regulates vascular morphogenesis of the *Arabidopsis* root. Genes Dev. **14**:2938–2943.

Mähönen, A.P., Bishopp, A., Higuchi, M., Nieminen, K.M., Kinoshita, K., Törmäkangas, K., Ikeda, Y., Oka, A., Kakimoto, T., and Helariutta, Y. (2006a). Cytokinin Signaling and Its Inhibitor AHP6 Regulate Cell Fate During Vascular Development. Science **311**:94–98.

Mähönen, A.P., Higuchi, M., Törmäkangas, K., Miyawaki, K., Pischke, M.S., Sussman, M.R., Helariutta, Y., and Kakimoto, T. (2006b). Cytokinins Regulate a Bidirectional Phosphorelay Network in Arabidopsis. Curr. Biol. **16**:1116–1122.

Mantovani, A., Locati, M., Vecchi, A., Sozzani, S., and Allavena, P. (2001). Decoy receptors: a strategy to regulate inflammatory cytokines and chemokines. Trends Immunol. **22**:328–336.

McMahan, C.J., Slack, J.L., Mosley, B., Cosman, D., Lupton, S.D., Brunton, L.L., Grubin, C.E., Wignall, J.M., Jenkins, N.A., and Brannan, C.I. (1991). A novel IL-1 receptor, cloned from B cells by mammalian expression, is expressed in many cell types. EMBO J. **10**:2821–2832.

Meyer, R.D., Mohammadi, M., and Rahimi, N. (2006). A Single Amino Acid Substitution in the Activation Loop Defines the Decoy Characteristic of VEGFR-1/FLT-1. J. Biol. Chem. **281**:867–875.

Michniewicz, M., Frick, E.M., and Strader, L.C. (2015). Gateway-compatible tissue-specific vectors for plant transformation. BMC Res. Notes **8**:63.

Miyawaki, K., Tarkowski, P., Matsumoto-Kitano, M., Kato, T., Sato, S., Tarkowska, D., Tabata, S., Sandberg, G., and Kakimoto, T. (2006). Roles of *Arabidopsis* ATP/ADP isopentenyltransferases and tRNA isopentenyltransferases in cytokinin biosynthesis. Proc. Natl. Acad. Sci. USA **103**:16598–16603.

Müller, B., and Sheen, J. (2008). Cytokinin and auxin interaction in root stem-cell specification during early embryogenesis. Nature **453**:1094–1097.

Rajeevkumar, S., Anunanthini, P., and Sathishkumar, R. (2015). Epigenetic silencing in transgenic plants. Front. Plant Sci. **6**:693.

Re, F., Muzio, M., Giri, J.G., Mantovani, A., and Colotta, F. (1994). The Type H "Receptor" As a Decoy Target for Interleukin 1 in Polymorphonuclear Leukocytes: Characterization of Induction by Dexamethasone and Ligand Binding Properties of the Released Decoy Receptor. J. Exp. Med. **179**:739–743.

Riefler, M., Novak, O., Strnad, M., and Schmülling, T. (2006). *Arabidopsis* Cytokinin Receptor Mutants Reveal Functions in Shoot Growth, Leaf Senescence, Seed Size, Germination, Root Development, and Cytokinin Metabolism. Plant Cell **18**:40–54.

Romanov, G.A., Spíchal, L., Lomin, S.N., Strnad, M., and Schmülling, T. (2005). A live cell hormone-binding assay on transgenic bacteria expressing a eukaryotic receptor protein. Anal. Biochem. **347**:129–134.

Sakai, H., Aoyama, T., Bono, H., and Oka, A. (1998). Two-Component Response Regulators from Arabidopsis thaliana Contain a Putative DNA-Binding Motif. Plant Cell Physiol. **39**:1232–1239.

Sakakibara, H., Suzuki, M., Takei, K., Deji, A., Taniguchi, M., and Sugiyama, T. (1998). A response-regulator homologue possibly involved in nitrogen signal transduction mediated by cytokinin in maize. Plant J. **14**:337–344.

Sakakibara, H., Takei, K., and Hirose, N. (2006). Interactions between nitrogen and cytokinin in the regulation of metabolism and development. Trends Plant Sci. **11**:440–448.

Sauer, M., Paciorek, T., Benková, E., and Friml, J. (2006). Immunocytochemical techniques for whole-mount in situ protein localization in plants. Nat. Protoc. **1**:98–103.

Suzuki, T., Miwa, K., Ishikawa, K., Yamada, H., Aiba, H., and Mizuno, T. (2001). The Arabidopsis Sensor His-kinase, AHK4, Can Respond to Cytokinins. Plant Cell Physiol. **42**:107–113.

Takei, K., Sakakibara, H., Taniguchi, M., and Sugiyama, T. (2001). Nitrogen-Dependent Accumulation of Cytokinins in Root and theTranslocation to Leaf: Implication of Cytokinin Species that Induces GeneExpression of Maize ResponseRegulator. Plant Cell Physiol. **42**:85–93.

Takeuchi, J., Fukui, K., Seto, Y., Takaoka, Y., and Okamoto, M. (2021). Ligand–receptor interactions in plant hormone signaling. Plant J. **105**:290–306.

To, J.P.C., Haberer, G., Ferreira, F.J., Deruère, J., Mason, M.G., Schaller, G.E., Alonso, J.M., Ecker, J.R., and Kieber, J.J. (2004). Type-A Arabidopsis Response Regulators Are Partially Redundant Negative Regulators of Cytokinin Signaling[W]. Plant Cell **16**:658–671.

To, J.P., Deruère, J., Maxwell, B.B., Morris, V.F., Hutchison, C.E., Ferreira, F.J., Schaller, G.E., and Kieber, J.J. (2008). Cytokinin Regulates Type-A *Arabidopsis* Response Regulator Activity and Protein Stability via Two-Component Phosphorelay. Plant Cell **19**:3901–3914.

Wang, Z., Ji, H., Yuan, B., Wang, S., Su, C., Yao, B., Zhao, H., and Li, X. (2015). ABA signalling is fine-tuned by antagonistic HAB1 variants. Nat. Commun. **6**:8138.

Wendrich, J.R., Yang, B., Vandamme, N., Verstaen, K., Smet, W., Van de Velde, C., Minne, M., Wybouw, B., Mor, E., Arents, H.E., et al. (2020). Vascular transcription factors guide plant epidermal responses to limiting phosphate conditions. Science **370**:eaay4970.

Werner, T., and Schmülling, T. (2009). Cytokinin action in plant development. Curr. Opin. Plant Biol. **12**:527–538.

Werner, T., Köllmer, I., Bartrina, I., Holst, K., and Schmülling, T. (2006). New Insights into the Biology of Cytokinin Degradation. Plant Biol. **8**:371–381.

Wulfetange, K., Lomin, S.N., Romanov, G.A., Stolz, A., Heyl, A., and Schmülling, T. (2011). The Cytokinin Receptors of Arabidopsis Are Located Mainly to the Endoplasmic Reticulum. Plant Physiol. **156**:1808–1818.

Yamada, H., Suzuki, T., Terada, K., Takei, K., Ishikawa, K., Miwa, K., Yamashino, T., and Mizuno, T. (2001). The Arabidopsis AHK4 Histidine Kinase is a Cytokinin-Binding Receptor that Transduces Cytokinin Signals Across the Membrane. Plant Cell Physiol. **42**:1017–1023.